博士論文

Integrin CD11b provides a new marker of IgA^+ B cells entering germinal centers in murine Peyer's patches

（インテグリンCD11bは、マウスパイエル板の胚中心に移行するIgA^+ B細胞の新しいマーカーである）

高　鵬

Table of contents

Chapter 1 Introduction **3**

Chapter 2 Materials and methods **10**

Chapter 3 Results **17**

Chapter 4 Discussion **42**

Chapter 5 Acknowledgement **47**

Chapter 6 References **48**

Chapter 1 Introduction

1-1 Antibody and immunoglobulin

In the 1890s, Emil von Behring and Shibasaburo Kitasato discovered the specific protein in the serum of animals. This specific protein, antibody, can bind specifically to the toxin and neutralize its activity. The substance, the antigen, can be recognized by the immune system and stimulate antibody generation. In response to the antigen, B cells express immunoglobulin (Ig) as B-cell receptor (BCR) on the membrane. Antibodies are the secreted form of the BCR produced by terminally differentiated B cells, which are also known as plasma cells (PCs).

Antibody (or Ig) is a Y shape protein containing 2 heavy chains and 2 light chains (Figure 1). Each heavy-chain and light-chain have a variable region and a constant region. The variable regions contain antigen-binding sites. Each antibody (or Ig) recognizes a specific structure of antigen (Figure 1). The strength of the antibody (or Ig) binding to the recognized antigen is called affinity. The constant region of the heavy chain determines the isotype of antibodies (Ig), such as IgM, IgD, IgG, IgE and IgA.

The antibody repertoire is large enough to ensure that there are antigen-binding sites that correspond to almost all potential antigens, albeit with low affinity. To neutralize and eliminate invading pathogens, B cells must produce and secrete high-affinity, different isotypes of antibodies. After stimulation by antigen, B cells can undergo Ig gene diversification processes, including somatic hypermutation (SHM) and class switch recombination (CSR)[1]. SHM introduces many point mutations in the variable region of Ig gene, which change the Ig affinity to the cognate antigen[1,2]. Also, the B cells change their Ig isotypes via CSR by changing their Ig constant region without changing the antigen-binding site[1,3]. Both the SHM and CSR contribute to the antibody (Ig) diversification for protecting the host from invading pathogens.

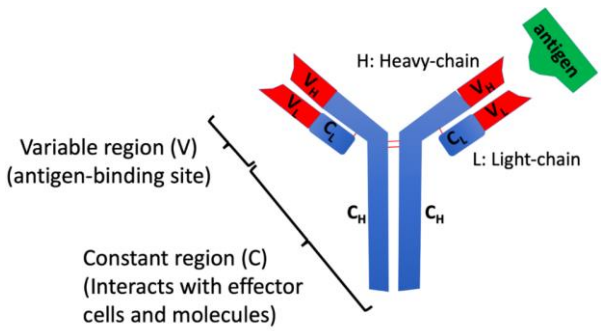

Figure 1 Structure of antibody

1-2 Germinal center (GC) reaction and vaccination

SHM occurs only in a transient structure called germinal center (GC)[4,5]. Only a small population of activated B cells can go into GC for SHM and affinity maturation and finally differentiate into high-affinity antibody-producing PCs[4,5].

B cells activated by antigens undergo three different pathways to differentiate into PCs[5,6]. First, some B cells are stimulated by antigen in a T cell-independent way, and soon differentiate into low-affinity short-lived PCs[5,6] (a in Figure 2). Second, the other antigen-activated B cells establish stable interaction with primed T cells in the interfollicular (IF) area. After T-B interaction, they differentiate into extrafollicular low-affinity short-lived PCs[5,6] (b in Figure 2). Third, the other small population of activated B cells enter the GC as pre-GC B cells with cognate T_H cells (c in Figure 2)[4-6]. Then, SHM and affinity maturation occurs in GCs and the affinity-selected B cells finally differentiate into high-affinity antibody-producing PCs or memory B cells. Memory B cells can reenter GC upon the antigen activation[5,7].

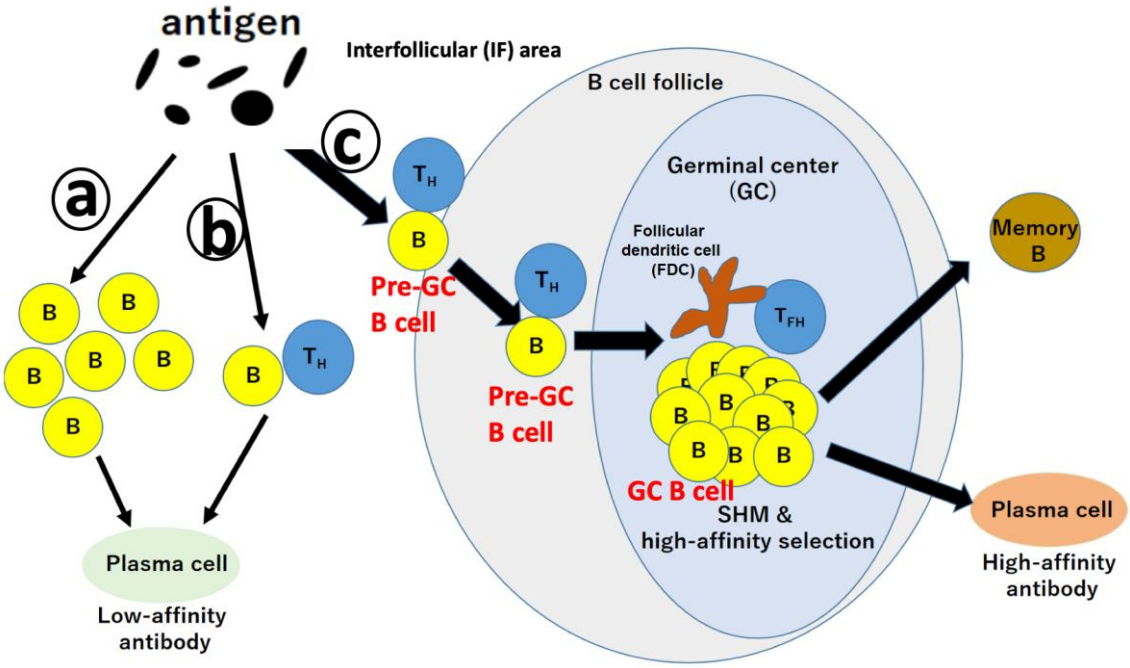

Figure 2 Generation of high-affinity antibody-producing plasma cells

(**a**) B cells are differentiated into low-affinity PCs via T-independent manner. (**b**) B cells are differentiated into low-affinity PCs via T-dependent manner. (**c**) B cells enter GCs and differentiate into high-affinity PCs via T-dependent manner.

GCs contain dark zones (DZs) and light zones (LZs) (Figure 3)[4]. Pre-GC B cells, derived from activated naïve B cells or memory B cells, enter GCs together with the primed T cells [4,5] (Figure 2). After entering GCs, pre-GC B cells enter the DZ of GC and turn to GC DZ B cells[4,5], while the T cells move into the LZ of GC as T follicular helper (T_{FH}) cells (Figure 3). GC DZ B cells begin to proliferate and undergo SHM, which generates a massive number of B-cell progenies with various mutations in their Ig genes (encoding BCR) and different affinities to the cognate antigen[2,4,5]. After the transition of B cells with mutations from DZ to LZ, they become GC LZ B cells. GC LZ B cells with high affinities take advantages to be positively selected as post-GC B cells and further differentiate into high-affinity PCs or memory B cells as shown in Figure 3 [4,5]. Unselected LZ B cells (low-affinity) can re-enter into the DZ, proliferate and undergo SHM to generate higher affinity antibodies[4,5,8] (Figure 3).

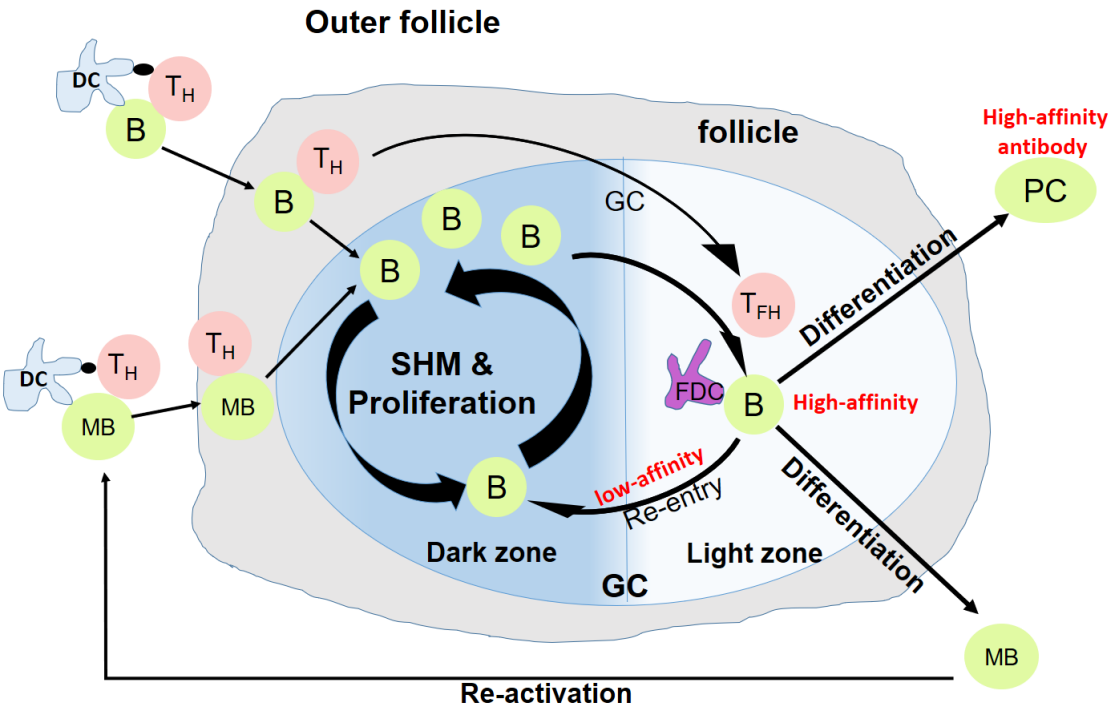

Figure 3 GC reaction

MB: memory B cell; T_{FH}: follicular T helper cell; PC: plasma cell; DC: dendritic cell;

FDC: follicular dendritic cell

Vaccination is a powerful application to induce antigen-specific high-affinity antibodies. Indeed, to evaluate the quality of a vaccine is based on whether it can effectively induce antibody immune response to generate high-affinity long-lived PCs and memory B cells for protection from the invading pathogens[9,10]. Therefore, research into the behavior of B cells and GC reaction during immune responses has been motivated by the potential benefit to vaccine development. The generation of those high-affinity long-lived PCs and memory B cells specifically rely on SHM during GC reaction in peripheral lymphoid tissues, including spleen, lymph nodes and Peyer's patches (PPs)[4]. As described above, only a small population will enter GC as pre-GC B cells for differentiation into high-affinity PCs. Therefore, pointing out the pre-GC B cells is helpful for the development of vaccine. However, at present, there is no specific surface marker to identify pre-GC B cells.

1-3 Intestinal immune response

The gut-associated lymphoid tissue (GALT) is the main site of the mucosal immune system, which contains organized structures, such as PPs, isolated lymphoid follicles and diffusely scattered lymphoid cells in the intestinal lamina propria (iLP) (Figure 4). In mucosal immune system, IgA is the main Ig isotype working as a microbial regulator as well as host defence against the invading pathogens[7,11,12]. In GALT, IgA is produced by PCs within iLP and secreted into the gut lumen through epithelial cells[11].

Based on the strength of binding to a recognized antigen, intestinal IgA can be classified into two types: low-affinity IgA and high-affinity IgA[7,11]. Intestinal high-affinity IgA-producing PCs are originated from the IgA^+ B cells in PPs through GC reaction[6,7] (Figure 4). As described above, within GC, B cells proliferate and change their BCR affinity through SHM, which is induced by an enzyme called activation-induced cytidine deaminase (AID)[1,2]. The study about AID^{G23S} mice, which lacks high-affinity IgA due to SHM defect, demonstrated that high-affinity IgA is important to regulate gut microbiota and protect the host against invading pathogens effectively[13]. Also, the study about high-affinity monoclonal intestinal IgA elucidated that an orally-administrated high-affinity IgA modulated gut microbiota by distinguishing harmful bacterial such as *Escherichia coli* from beneficial bacteria like *Lactobacillus casei*[14]. These studies indicate that high-affinity, but not low-affinity, IgA is crucial for mucosal immunity.

PPs are good sites to be focused on the mechanism of GC reaction, since the B cells in PPs are constitutively stimulated by the antigens in the gut lumen. PPs always contain pre-existing GCs[12,15] while other lymphoid organs such as spleen and lymph nodes do not. Therefore, we can find pre-GC B cells that are entering the existing GCs at any time point without immunization in PPs[12,15].

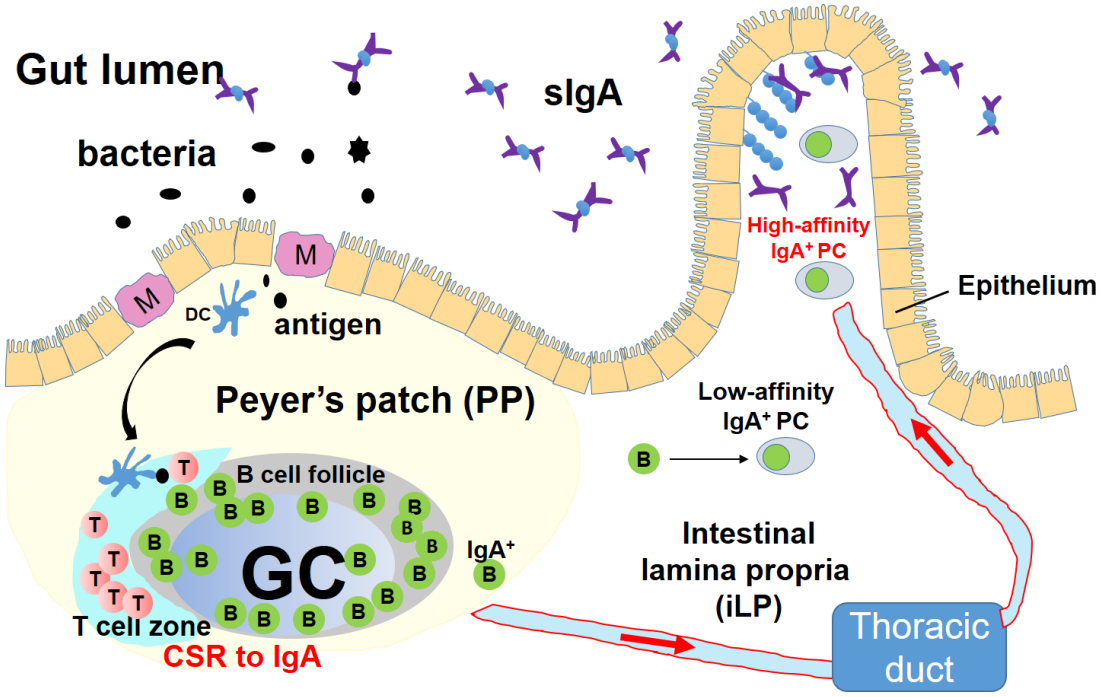

Figure 4 Intestinal high-affinity IgA$^+$ PCs are derived from B cells in PPs

1-4 Integrin CD11b and B cells

CD11b, the 165-kDa integrin alpha M, associates with CD18 to form heterodimeric integrin known as macrophage-1 antigen (Mac-1), which binds to the intercellular adhesion molecule 1 (ICAM-1)[16] (Figure 5). Integrin is a transmembrane receptor involved in regulating cell adhesion and migration. As integrin, CD11b is widely considered as a marker for myeloid cells[16]. However, some B cells, especially B1 cells in murine peritoneal cavity (PerC), express CD11b on their surface, although its function has not been classified[17].

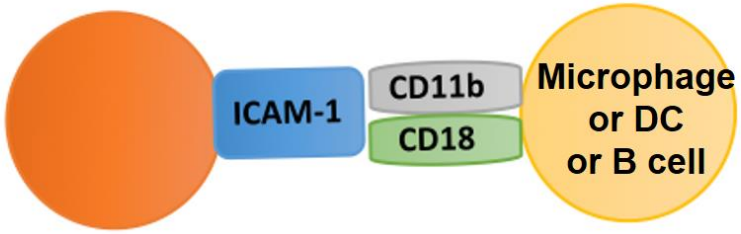

Figure 5 Integrin CD11b

Recent studies about CD11b knockout mice demonstrated a complex function of CD11b on B cells[18.19]. Ding *et al.* have shown that CD11b negatively regulates BCR signaling to maintain autoreactive B cell tolerance[18]. GC B cell response in CD11b-knockout mice is hyperproliferative, which may result in autoimmunity[18,19]. Indeed, human genetic variations in the *ITGAM* gene (encoding CD11b) strongly associate with risk for systemic lupus erythematosus (SLE)[20]. These studies indicated that the enhancement of GC reaction is not always beneficial. Therefore, not only enhancing GC reaction but also properly regulated GC reaction is important for future vaccine development. Therefore, we thought that CD11b may play an important role for controlling the GC reaction.

On the other hand, to initiate the GC reaction, efficient activation of dendritic cells (DCs) has been reported to be essential[21,22]. Therefore, many previous studies focus on selecting the most appropriate adjuvant to stimulate DCs[21,22]. However, Lycke and co-workers have demonstrated that PP B cells can sample antigen from microfold (M) cells and further migrate into GCs in mice depleted of DCs[23], indicating that DC activation is not necessary for GC entry in PPs. Even though DCs are properly primed, only a small population of activated B cells can develop into pre-GC B cells and enter the GC. Thus, which population of activated B cells is pre-GC B cells entering GC is a valuable question for improving the development of vaccine. One recent study has reported that a transcription factor essential for GC formation, *irf4*, which is highly expressed in pre-GC B cells, is a candidate pre-GC B cell marker[24]. However, there is no known specific surface marker for pre-GC B cells. Hence the criteria for pre-GC B cells, and which kinds of activated B cells enter GCs to produce high-affinity BCR against a specific antigen are not well understood.

1-5 Our question, hypothesis and study

Here, we address two questions. Which population of B cells are pre-GC B cells entering GCs to produce high-affinity antibodies? And what stimulation can induce pre-GC B cells in order to enhance the GC reaction? As we described above, since integrin CD11b may play an important role in regulating the GC reaction, we hypothesized that $CD11b^{+}IgA^{+}$ B cells are pre-GC B cells in PPs.

In the present study, we identified a small population of IgA^{+} B cells expressing integrin CD11b as pre-GC B cells, located outside of GCs and highly expressed *irf4*, in murine PPs. After injection of the $CD11b^{+}IgA^{+}$ PP B cells into a PP of IgA-Cre/YC3.60^{flox} reporter mice, the injected cells did not enter existing GCs directly but located surrounding of GCs, and then they entered the GCs forty-hours later, indicating that they are pre-GC IgA^{+} B cells in murine PPs. Furthermore, we found that some bacterial antigens including pam3CSK4, lipopolysaccharide (LPS) and heat-killed *Escherichia coli* (*E. coli*) or *Salmonella enterica* (*S. enterica*), but not *Bifidobacterium*, induced CD11b expression in naïve B cells *in vitro*. The CD11b expression on B cells before T-B or DC-B interaction allowed the intravenously-injected B cells to enter existing GCs in PPs. Thus, B cells control their own cell fate to become pre-GC B cells, which is independent of DC activation. In addition, mice orally administered with pam3CSK4 or heat-killed *E. coli* increased the number of PP GC B cells within two days, and enhanced the mucosal antigen-specific IgA response. We propose that the induction of CD11b on activated B cells is a promising marker of pre-GC B cells as well as a useful criterion for selecting an effective mucosal vaccine adjuvant.

Chapter 2 Material and method

Mice

Balb/c mice (at 8-12 weeks old) were obtained from Japan CLEA. Mice were bred and maintained under specific pathogen-free conditions at the Animal Facility of the Institute for Quantitative Bioscience (IQB), the University of Tokyo. All experiments were performed following the guidelines of the Animal Care and Use Committee of IQB, the University of Tokyo.

For transfer experiments of B cells, we used IgA-Cre/YC3.60^{flox} mice (8-12 weeks-old) generously provided by Dr. T. Adachi, Tokyo Medical and Dental University. Briefly, IgA-Cre mice were designed based on Cris Allen's paper[25]. After crossing with YC3.60^{flox} mice[26,27], IgA^{+} cells are identified as YC3.60^{+} cells.

Flow cytometry analysis and Cell sorting

PPs were carefully excised from the small intestine of Balb/c mice. Single-cell suspensions prepared from PPs were incubated with combinations of the following antibodies: Phyacoerythrin-Cy7 (PE-cy7) anti-mouse/human B220 (eBioscience mAb RA3-6B2), PE anti-mouse/human B220 (Biolegend mAb RA3-6B2), FITC anti-mouse/human B220 (Biolegend mAb RA3-6B2), PE anti-mouse IgA (alpha chain specific) (Southern Biotech), Alexa Fluor (AF) 647 anti-mouse IgA (Southern Biotech), FITC anti-mouse CD11b (Biolegend mAb M1/70), PE anti-mouse CD11b (Biolegend mAb M1/70), PE-cy7 anti-mouse CD11b (eBioscience mAb M1/70), Biotinylated PNA (Vector Laboratories), APC-R700 Hamster anti-mouse CD95 (Fas) (BD Biosciences mAb Jo2), AF488 anti-mouse CD86 (Biolegend mAb GL-1), APC anti-mouse CD184 (CXCR4 mAb L236F12) (Biolegend), PE anti-mouse IgM (eBiosciences mAb eB121-15F9), AF647 anti-mouse CD4 (Biolegend mAb GK1.5), streptavidin PE (Biolegend), streptavidin APC (Biolegend), streptavidin AF488 (Lifetechnologies). FSC-H/FSC-W gate was used to select the singlet cells. Propidium iodide (PI) was used to exclude dead cells. Flow cytometry analysis was performed with Spectral Cell Analyzer SA3800 (SONY). Cell sorting was performed with Cell Sorter SH800 (SONY).

Immunohistochemical analysis

Freshly isolated Peyer's patches were snap-frozen in Optimum Cutting Temperature (OCT) compound (Sakura Finetechnical) and stored at −80 ℃. PP sections with a thickness of 6 μm were prepared and dried overnight. On the next day, PP sections were fixed for 10 minutes at -20 °C in acetone (Nacalai). After washing with phosphate-buffered saline (PBS) 5 times, the sections were then incubated in blocking

buffer (PBS/5% FCS (NICHIREI BIOSCIENCES INC.)) for 30 minutes. PP sections were then incubated for more than 30 minutes at RT in a dark box with the combination of the following antibodies: AF488 anti-mouse/human CD11b (Biolegend mAb M1/70), PE anti-mouse/human CD11b (Biolegend mAb M1/70), AF488 anti-mouse CD4 (Biolegend mAb GK1.5), AF647 anti-mouse CD4 (Biolegend mAb GK1.5), DAPI solution (BD Bioscience), AF488 anti-mouse CD54 (ICAM-1) (Biolegend mAb YN1/1.7.4), AF647 anti-mouse CD54 (ICAM-1 mAb YN1/1.7.4) (Biolegend), Biotin anti-mouse CD11c (eBioscience mAb N418), AF488 anti-mouse MAdCAM-1 (Biolegend mAb MECA-367), PE anti-mouse MAdCAM-1 (Biolegend mAb MECA-367), Biotinylated PNA, AF647 anti-mouse IgA (alpha chain specific) (Southern Biotech), PE anti-mouse IgA (alpha chain specific) (Southern Biotech), streptavidin AF488 (Lifetechnologies). Sections were observed under microscopy LSM880 (Carl Zeiss). Images were analyzed with software of ZEN2009 (Carl Zeiss).

RNA purification and real-time PCR

Roughly 1 x 10^4 PP GC B cells ($PNA^{hi}B220^+$ cells) and 1 x 10^4 non-GC PP B cells ($PNA^{lo}B220^+$) were sorted, respectively. RNA was extracted from sorted cells with NucleoSpin RNA XS (Takara). cDNA was synthesized with GoScript™ Reverse Transcriptase (Promega). Real-time PCR was performed in triplicate on 384-well optical PCR plates (Roche) with KAPA SYBR® FAST qPCR Master Mix (2X) Kit (KAPA Biosystems) on LightCycler 480 (Roche). Gene expression levels were normalized with the expression level of housekeeping gene *β-actin*. The following primers were utilized for analysis. *β-actin* fw: 5'-CCAACCGTGAAAAGATGACC-3', *β-actin* rv: 5'-CCAGAGGCATACAGGGACAG-3', *itgam* (CD11b) fw: 5'-CAGATCAACAATGTGACCGTATGGG-3', *itgam* (CD11b) rv: 5'-CATCATGTCCTTGTACTGCCGCTTG-3', *aicda* (AID) fw: 5'-CCTACGCTACATCTCAGACT-3', *aicda* (AID) rv: 5'-CTTTGAAGGTCATGATCCCG-3', *bcl6* (BCL6) fw: 5'-TCCTCACGGTGCCTTTTTACA-3', *bcl6* (BCL6) rv: 5'-TAACGACAAGCATGACGCAG-3', *irf4* (IRF4) fw: 5'-AGGTCTGCTGAAGCCTTGGC-3', *irf4* (IRF4) rv: 5'-CTTCAGGGCTCGTCGTGGTC-3', *s1pr2* (S1PR2) fw: 5'-GTGACGGGACGCAGAGGT-3', *s1pr2* (S1PR2) rv: 5'-AAATGTCGGTGATGTAGGCATATG-3', *bcl2* (BCL2) fw: 5'-TGAGTACCTGAACCGGCATCT-3', *bcl2* (BCL2) rv: 5'-GCATCCCAGCCTCCGTTAT-3', *gpr183* (EBI2) fw: 5'-GACATCCTGTTTACCACAGCT-3', *gpr183* (EBI2) rv: 5'-AGACCAGAATCCAGACGGACA-3'.

Microarray analysis

RNA was separately extracted from 25,000 sorted $CD11b^+IgA^+$ B cells and 100,000 sorted $CD11b^-IgA^+$ B cells with NucleoSpin RNA XS (Takara, Japan). Microarray analysis was performed with SurePrint G3 Mouse GE v2 8x60K Microarray Chip (Affymetrix) to detect the gene expression.

***In vivo* Imaging**

For migration imaging, IgA-Cre/YC3.60^{flox} mice (8-12 weeks-old) were anesthetized with a mixture of three types of anesthetic agents as described[28]. An incision was carefully made in the abdominal wall, and the small intestine was exposed. PPs were identified by naked eyes. About 8,000 sorted $CD11b^+IgA^+$ PP B cells and 30,000 $CD11b^-IgA^+$ PP B cells were labeled with CellTracker Orange CMTMR fluorescent dye (Invitrogen) and then injected to a PP of IgA-Cre/YC3.60^{flox} mice transgenic mouse directly by a 25 μL syringe (Trajan Scientific and Medical). The PP with transferred cells was observed under an LSM 880 microscope (Carl Zeiss). Images were analyzed with ZEN2009 software (Carl Zeiss). After one hour observation of the PP under a microscope, the abdominal incision was carefully closed with an ELP Skin Stapler (Akiyama Co. Ltd.). Forty hours after transfer, under anesthesia, the PP with transferred cells was observed again to identify the localization of transferred $CD11b^+IgA^+$ PP B cells under an LSM 880 microscope (Carl Zeiss) and analyzed with ZEN2009 software (Carl Zeiss).

Conjugation analysis

Conjugations between $CD11b^+IgA^+$ PP B cells and $CD4^+$ PP T cells were analyzed by flow cytometry with Cell Sorter SH800 (SONY). Singlet cells were selected by FSC-H/FSC-W gate. Conjugated cells were negatively selected by discrimination of the singlet cell gate. For imaging, the conjugated cells were sorted from PP conjugated $CD11b^+IgA^+CD4^+$ gate and observed with microscopy LSM880 (Carl Zeiss) and analyzed software of ZEN2009 (Carl Zeiss)**.**

Sorted $CD11b^+IgA^+$ PP B cells on induced GC-like B cell (iGB) culture system

About 800 sorted $CD11b^+IgA^+$ PP B cells and 800 sorted $CD11b^-IgA^+$ PP B cells were stained with CellTrace Violet Proliferation Kit (Invitrogen). Since the number of sorted $CD11b^+IgA^+$ PP B cells was very small, 5,000 $CD11b^-IgA^+$ PP B cells and 5×10^4 naïve spleen B cells (negatively sorted by B cell isolation kit (Miltenyi Biotec)) were prepared as positive controls. To monitor cell proliferation, the sorted $CD11b^-IgA^+$ PP B cells, $CD11b^+IgA^+$ PP B cells and naïve spleen B cells were seeded in a 6-well

tissue culture dish in the presence of 40LB cells[29] that have been pre-treated with mitomycin C to inhibit the growth. Cells were cultured in RPMI-1640 medium (Wako) (containing 10% FCS, 5.5×10^{-5} M 2-Mercaptoethanol (ME) (Nacalai), 10 mM HEPES (Nacalai)) at 37℃ with 5% CO_2 for 3 days. Sorted $CD11b^{+}IgA^{+}$ PP B cells and $CD11b^{-}IgA^{+}$ PP B cells were cultured with rIL-21 (10 ng/ml; PeproTech) and naïve spleen B cells were cultured with rIL-4 (1 ng/ml; Biolegend). Flow cytometry analysis was performed to detect CellTrace Violet from day 0 to day 3 with the iGB culture system. CD11b expression of culturing cells were analyzed on day 0 and day 1 by flow cytometry with Cell Sorter SH800 (SONY) and Spectral Cell Analyzer SA3800 (SONY).

Pam3CSK4-stimulated spleen $CD11b^{+}$ B cells on iGB culture system

For the spleen $CD11b^{+}$ B cells culture on iGB culture system, spleen naïve B cells were cultured with pam3CSK4 (Invivogen) for 3 days to induce CD11b expression. Then, 1.5×10^5 $CD11b^{+}$ spleen B cells and 1.5×10^5 $CD11b^{-}$ spleen B cells were sorted by flow cytometry and stained with CellTrace Violet (Invitrogen), and then subsequently cultured on 40LB system with IL-4 (1ng/ml; Biolegend) for 4 days. Their CD11b expressions were then analyzed by flow cytometry with Cell Sorter SH800 (SONY) and Spectral Cell Analyzer SA3800 (SONY).

Bacteria preparation for B cell stimulation

E. coli (DH5α) and *S. enterica* were inoculated from a glycerol stock into 5 ml of LB medium and then cultured by shaking at 180 rpm for overnight at 37 ℃. On the second day, 0.5 ml of the cell suspension was resuspended in 10 ml of LB medium. The culture was grown at 37 ℃ with shaking (180 rpm) for 3 h. The growth curve of the culture was monitored by the optical density (OD) at the wavelength of 600nm (OD600) detected every 30 minutes. One hundred μl of serial dilutions of cell suspension were spread onto LB plate to calculate CFU. Based on growth curve, we cultured, harvested *E. coli* and *S. enterica* and heat-killed them by autoclaving (121℃, 15 minutes).

Similarly, *B. bifidum* and *B. breve* were anaerobically cultured at 37℃ in Difico Lactobacilli MRS broth (Becton, Dickinson and Company) medium, and heat-killed by autoclaving.

Spleen B cell stimulation *in vitro*

Spleen B cells were negatively sorted with B cell isolation kit (Miltenyi Biotec) from a spleen of 8-week-old Balb/c mice. Splenic B cells (with concentration: 5×10^5/ml) were cultured in RPMI1640 medium with 13 independent stimulations, respectively. To select the proper concentration of each stimulation, we show the results of titration of each stimulation.

1. Anti-mouse IgM (15 μg/ml; Jackson Immuno Research Laboratories)
2. Anti-mouse-CD40 (HM40-3, 500 ng/ml; Biolegend)
3. BAFF (50 ng/ml; Biolegend)
4. Pam3CSK4 (1 μg/ml, Invivogen)
5. Poly I:C (25 ng/ml, Invivogen)
6. LPS (50 ng/ml; Sigma-Aldrich)
7. Flagellin (20 ng/ml; Sigma-Aldrich)
8. Imiquimod (R837, 5 ng/ml; Invivogen)
9. CpG (20 ng/ml, GeneDsign Inc)
10. Heat-killed *E. coli* (10^7 CFU/ml)
11. Heat-killed *S. enterica* (10^8 CFU/ml)
12. Heat-killed *B. bifidum* (10^7 CFU/ml)
13. Heat-killed *B. breve* (10^7 CFU/ml)

CD11b expression of stimulated B cells was analyzed on day 0 and day 3 with Cell Sorter SH800 (SONY) and Spectral Cell Analyzer SA3800 (SONY).

For MDP stimulation, purified splenic B cells (5×10^5/ml) were cultured in RPMI1640 medium with N-acetylmuramyl-L-alanyl-D-isoglutamine hydrate (1 μg/ml; Sigma-Aldrich).

For TLR inhibitor and NOD2 inhibitor analysis, purified splenic B cells (5×10^5/ml) were cultured in RPMI1640 medium with TLR1/2 antagonist, CU-CPT (1 μM; Sigma-Aldrich), TLR4 inhibitor, TAK-242 (1 μM; Sigma-Aldrich) or NOD2 signaling inhibitor II, GSK717 (30 μM; Sigma-Aldrich) in the presence of pam3CSK4 (1 μg /ml, Invivogen), LPS (50 ng/ml; Sigma-Aldrich), CpG (20 ng/ml, GeneDsign Inc) and heat-killed *E. coli* (10^7 CFU/ml).

Immunization

On days 0 and 16, mice were orally administered with OVA (1 mg), OVA (1 mg) + pam3CSK4 (10 μg, Invivogen) or OVA (1 mg) + heat-killed *E. coli* (10^9 CFU in 100 μl). On day 21, feces were collected for OVA-specific antibody measurement by enzyme-linked immunosorbent assay (ELISA).

Detection of OVA-specific IgA ELISA

Feces were suspended in 10 times weight/volume (w/v) of PBS. After centrifugation (8,000g for 15 minutes), supernatant was collected as fecal extracts. Plates were pre-coated with 1 mg/ml OVA for overnight, and followed by blocking for 1 hour at room temperature with PBS containing 1% (w/v)

bovine serum albumin. Then fecal extracts with serial dilutions were added for incubation for 1 hour at room temperature. The relative binding ability of IgA was detected with alkaline phosphatase-conjugated goat anti-mouse IgA (Southern Biotech). After incubation at 4℃ overnight, the optical density (OD) values at 405nm were measured with TriStar Multimode Reader LB 942 (BERTHOLD).

Oral administration with heat-killed bacteria to WT mice

Balb/c mice (at 8-12 weeks old) were orally administered with heat-killed *E. coli* (10^9 CFU diluted by 100 μl PBS per mouse), *S. enterica* (10^9 CFU diluted by 100 μl PBS per mouse), *B. bifidum* (10^9 CFU diluted by 100 μl PBS per mouse), *B. breve* (10^9 CFU diluted by 100 μl PBS per mouse) and pam3CSK4 (10 μg diluted by 100 μl PBS per mouse). Mice orally administered with 100 μl PBS were prepared as controls. Two days later, PPs from those mice were prepared to analyze their GC B cells with Spectral Cell Analyzer SA3800 (SONY), as above described.

***In vivo* imaging of transferred iGB cells induced by pre-stimulation**

As described above, spleen naïve B cells were cultured with pam3CSK4 (1 μg/ml, Invivogen), heat-killed *E. coli* (10^7 CFU/ml), CpG (20 ng/ml, GeneDsign Inc) or anti-IgM-Ab (15 μg/ml; Jackson Immuno Research Laboratories) for 3 days *in vitro*, separately. Then, 1×10^5 $B220^+$ B cells were sorted from the simulated cells and subsequently seeded on 40LB feeder cells with rIL-4 (1 ng/ml; Biolegend) to induce iGB cells[29]. Non-stimulated spleen naïve B cells were seeded on 40LB feeder cells with rIL-4 (1 ng/ml; Biolegend) as control group.

After 4-day culturing, 3×10^5 iGB cells ($B220^+$) of naïve B-40LB cells, pam3CSK4-40LB cells, *E. coli*-40LB, IgM-40LB and CpG-40LB cells were sorted and labeled with CellTracker Orange CMTMR fluorescent dye (Invitrogen) and then separately injected intravenously to a mouse (Balb/c, 8-12 weeks old) together with 10 μg of AF488 anti-mouse MAdCAM-1 (Biolegend mAb MECA-367) to identify HEVs. Under anesthesia, to stain the IgA^+ cells for GC identification, 1 μg of AF647 anti-mouse IgA (Southern Biotech) was directly injected to a PP of the same mouse transferred with iGB cells. The localization of transferred labeled iGB cells was observed with microscopy LSM880 (Carl Zeiss) and analyzed software of ZEN2009 (Carl Zeiss)**.**

DNA amplification of rearranged VDJ region and downstream intron

Rearranged VDJ sequences with downstream intronic sequences were amplified by two rounds of nested PCR with several different upstream primers (where 'S' is C or G; 'R' is A or G; 'N' is A, G, C or T; 'M' is A or C; and 'W' is A or T): MH1, 5′-SARGTNMAGCTGSAGSAGTC-3′; MH2, 5′-

SARGTNMAGCTGSAGSAGTCWGG-3′; MH3, 5′-CAGGTTACTCTGAAAGWGTSTG-3′; MH4, 5′-GAGGTCCARCTGCAACARTC-3′; MH5, 5′-CAGGTCCAACTVCAGCARCC-3′; MH6, 5′-GAGGTGAASSTGGTGGAATC-3′; MH7, 5′-GATGTGAACTTGGAAGTGTC-3′, together with JH4R primer that is complementary to a sequence located at the 5'-end of the IgH intronic enhancer (5'-GACTAGTCCTCTCCAGTTTCGGCTGAATCC-3')[13,30]. The second round of PCR was carried out with the same upstream primers together with JH4R-2 primer (5'-CAGGTGGTGTTTTGCTCA-3') that is complementary to an upstream sequence of JH4R primer. Amplification was carried out with 20 cycles of first round PCR and 30 cycles of second round PCR (95℃ 15 sec, 58℃ 10 sec, 72℃ 30 sec) with PrimeSTAR Max DNA Polymerase (TaKaRa). After cloning the PCR products into pGEM T vector (Promega), clones containing the intronic sequence were selected by colony PCR with JH4F primer (5'-TAT GCT ATG GAC TAC TGG-3') and JH4R-2 primer with EmeraldAmp® PCR Master Mix (TAKARA).

DNA sequencing and SHM analysis

After plasmid DNA isolation, DNA sequence analysis was performed with T7 and SP6 primers. The consensus of IgH intronic DNA sequence was retrieved from the Accession No. AJ 851868.3. The rearranged VDJ was assigned with the IgBLAST.

Statistical analysis

Except when otherwise stated, statistical analyses were performed using GraphPad Prism version 8.4.2 for Mac (GraphPad Software, San Diego, CA, USA). Differences between two individual groups were compared using a two-tailed unpaired Student's *t* test. In the case of more than three groups, one-way or two-way analysis of variance (ANOVA) followed by Tukey's multiple comparisons test was performed. The statistical test and details about group number and replicates are indicated in the figure legends. A p value <0.05 was considered significant.

Chapter 3 Results

3-1 A small population of IgA$^+$ B cells expresses CD11b in murine PPs.

To find pre-GC B cells, we investigated the CD11b expression on IgA$^+$ B cells in PPs. By flow cytometry, we identified a small population of CD11b$^+$IgA$^+$ B cells in PPs (about 0.1% to 0.2% of PP B cells) (Figure 6). Since the number of IgA$^+$ B cells in PPs is not large (about 2 x 10^5 IgA$^+$ B cells per mouse), we thought that we should not ignore the population of CD11b$^+$IgA$^+$ B cells in PPs. Our finding suggests that IgA$^+$ B cells in PPs can be also divided into two populations, CD11b$^+$IgA$^+$ B cells and CD11b$^-$IgA$^+$ B cells.

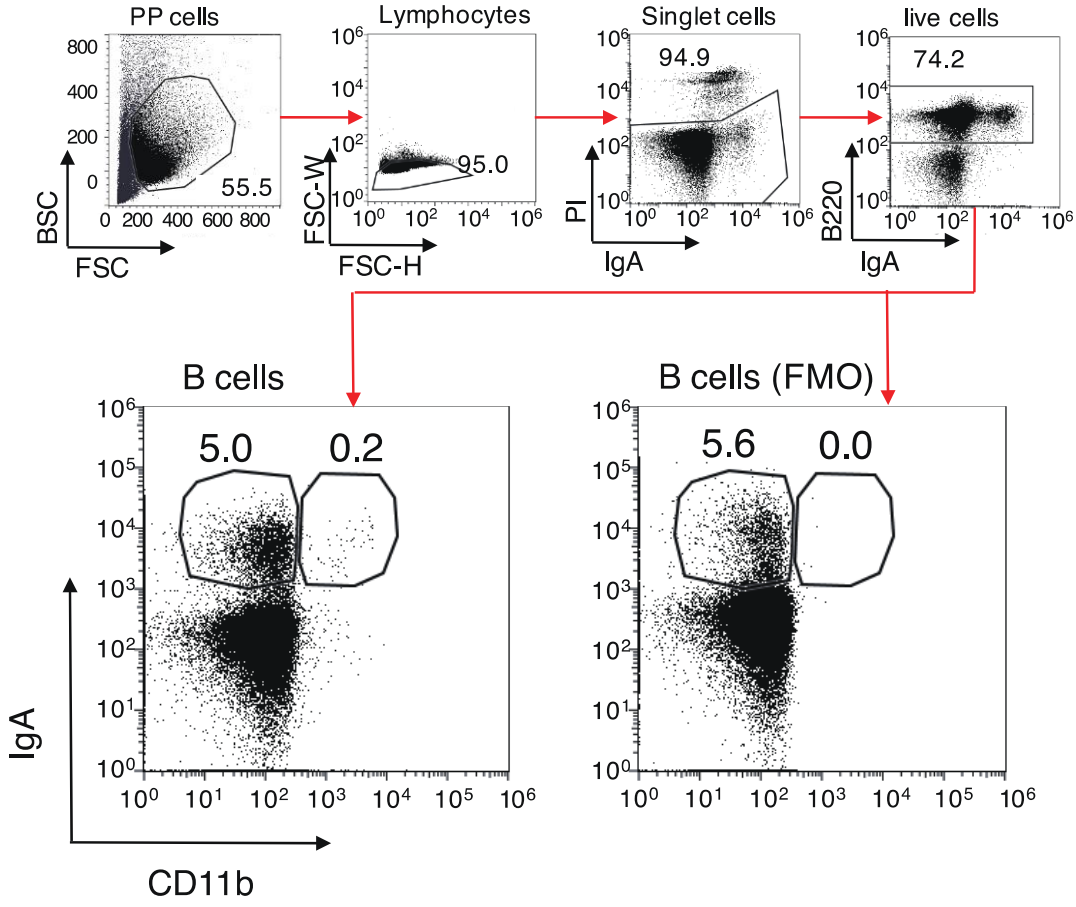

Figure 6 CD11b$^+$IgA$^+$ B cells exist in murine PPs.

Flow cytometry analysis was performed with WT mice of 8-12-week-old. Doublet cells were discriminated by FSC-H/FSC-W gate. Dead cells were excluded by PI staining. IgA and CD11b expressions were analyzed in the B220$^+$ B cells. Fluorescence minus one (FMO) samples were prepared

without CD11b staining as negative control. Representative data are from at least 20 independent experiments.

3-2 Both CD11b$^+$IgA$^+$ and CD11b$^-$IgA$^+$ PP B cells express typical GC surface markers.

To check if the CD11b$^+$IgA$^+$ and CD11b$^-$IgA$^+$ PP B cells are GC B cells, we further performed flow cytometry analysis with PNA and Fas, typical GC B cell markers[13]. As shown in Figure 7, more than 70% of CD11b$^+$IgA$^+$ PP B cells and CD11b$^-$IgA$^+$ PP B cells were PNA^{hi} phenotypes, and more than 80% of both of the two populations were Fas$^+$ B cells. These results suggested that both the CD11b$^+$IgA$^+$ and CD11b$^-$IgA$^+$ PP B cells are GC B cells.

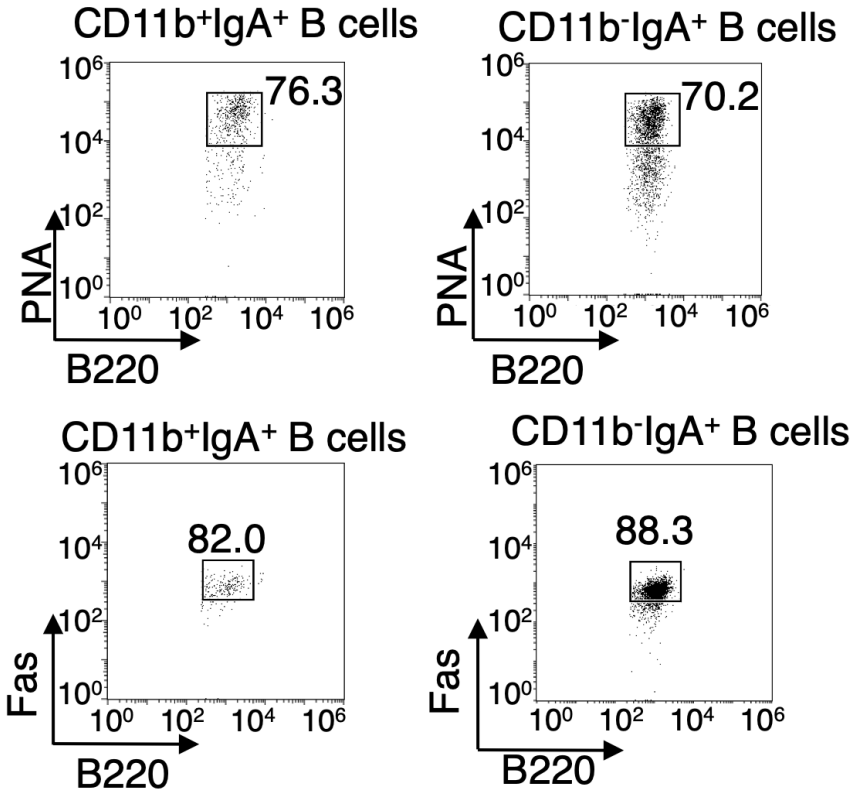

Figure 7 Both CD11b$^-$IgA$^+$ and CD11b$^+$IgA$^+$ PP B cells in PPs show GC cell phenotypes. Representative flow cytometry data of CD11b$^-$IgA$^+$ B cells and CD11b$^+$IgA$^+$ B cells in PPs for PNA and Fas expressions. Representative data are from at least five independent experiments.

3-3 CD11b$^+$IgA$^+$ B cells are located outside GC.

Then, we examine the localization of CD11b$^+$IgA$^+$ PP B cells, since pre-GC B cells are located in the IF area (outside GCs) before entering GCs[4,5]. As shown in Figure 8a, the GC area was

identified by PNA staining and IgA^+ cells-enriched area. As we expected, we did not find CD11b expression on IgA^+ B cells in GC (Figure 8a), We found that only two $CD11b^+IgA^+$ B cells (yellow cells) reside in the area outside the GC in the section (Figure 8a, b), which is a reasonable result because the number of $CD11b^+IgA^+$ B cells is very small.

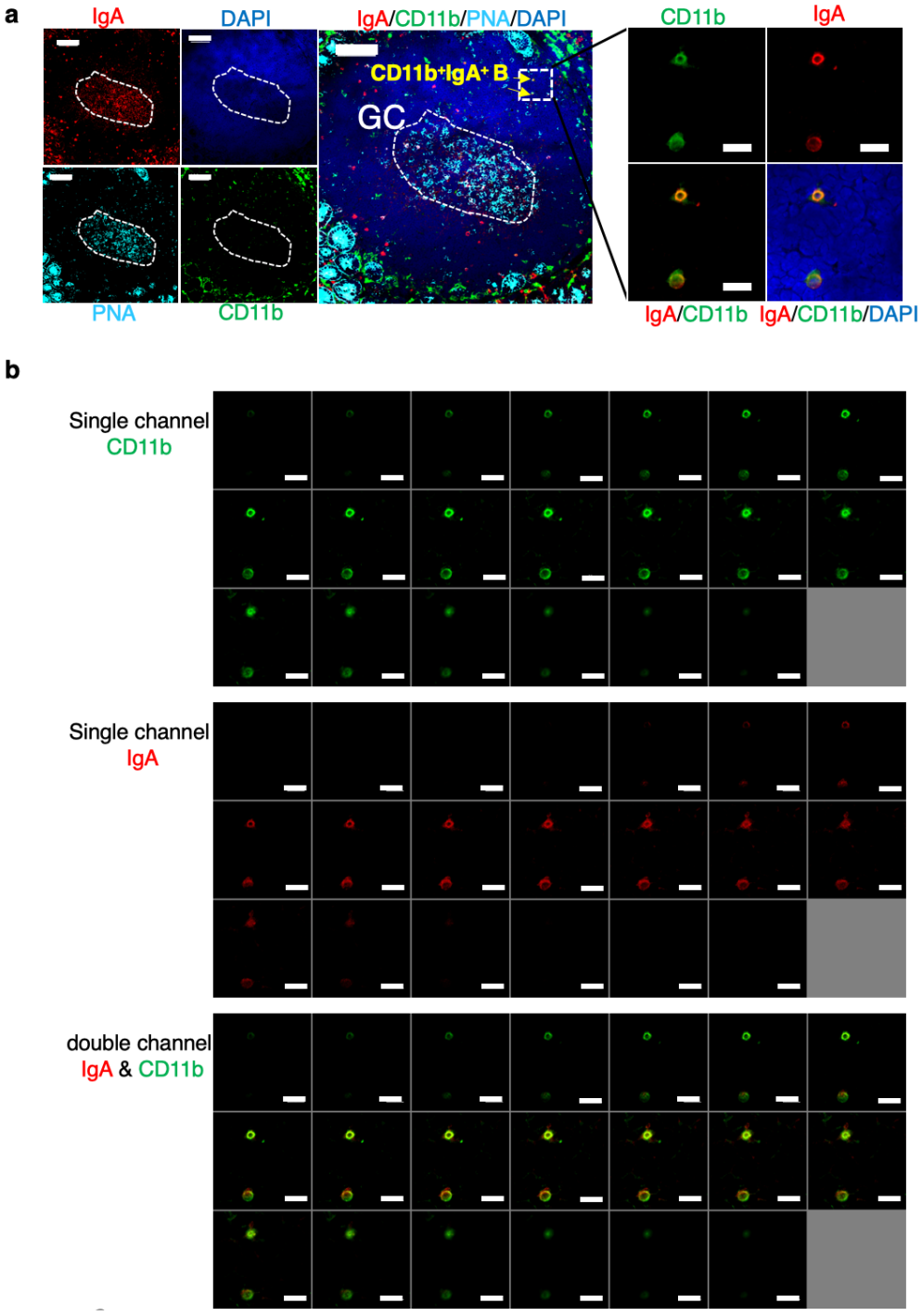

Figure 8 Localization analysis of $CD11b^+IgA^+$ B cells by immunohistochemistry.

(**a**) Representative microscopy images showed that $CD11b^{+}IgA^{+}$ PP B cells localized outside GC. PNA (cyan) was used to identify GC (dashed circle). Most IgA^{+} cells (red) were located in GC. $CD11b^{+}IgA^{+}$ (yellow arrow) double positive cells (yellow cells) were not detected in GC (dashed circle). DAPI (blue) was used to stain the nuclei. Scale bar, 100μm. (**b)** Z-stack analysis was performed with boxed area to confirm that the CD11b (green) and IgA (red) signals overlapped. Scale bar, 10 μm.

3-4 High-endothelial venules (HEVs) express intercellular adhesion molecular-1 (ICAM-1), the ligand of CD11b, in IF area in PPs.

We subsequently analyzed the localization of the CD11b ligand. ICAM-1 is widely known as the ligand of CD11b/CD18 that mediates cell adhesion and migration [16,31]. As reported previously [8,32], both GC B cells and high endothelial venules (HEVs) in IF area express ICAM-1 (Figure 9a, b). The HEVs also express mucosal addressin cell adhesion molecule-1(MAdCAM-1)[32].

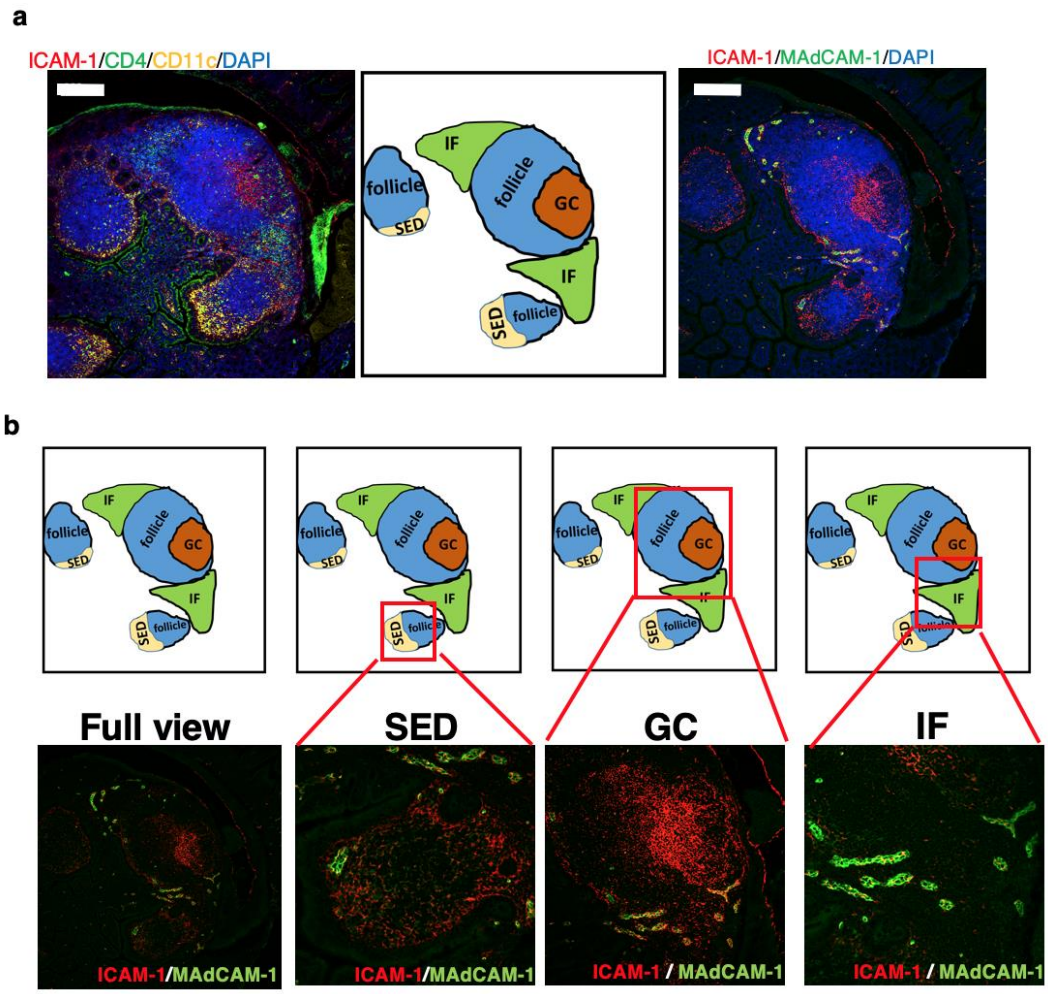

Figure 9 ICAM-1, the ligand of CD11b, is highly expressed in GC and HEVs.

(a) Representative microscopy images showed the SED, IF, GC areas stained with ICAM-1 (red), CD11c (yellow, left), CD4 (green, left), MAdCAM-1 (green, right) and DAPI. Each area was marked in the middle schema. Scale bar, 200μm (**b)** Boxed areas were amplified to show ICAM-1and MAdCAM-1 co-localization.

3-5 CD11b$^+$IgA$^+$ PP B cells are located in IF area near HEVs.

Next, we analyzed the localization of CD11b$^+$ IgA$^+$ PP B cells again to check whether they are binding to the HEVs. Although we did not find the CD11b$^+$IgA$^+$ PP B cells directly binding to HEVs, we found 6 out of 7 CD11b$^+$IgA$^+$ PP B cells were located near HEVs in the IF area in a section of PPs (Figure 10). Another CD11b$^+$IgA$^+$ PP B cell (No.7) was located near the GC (Figure 10), but not inside GC, suggesting that it is migrating to GC from IF.

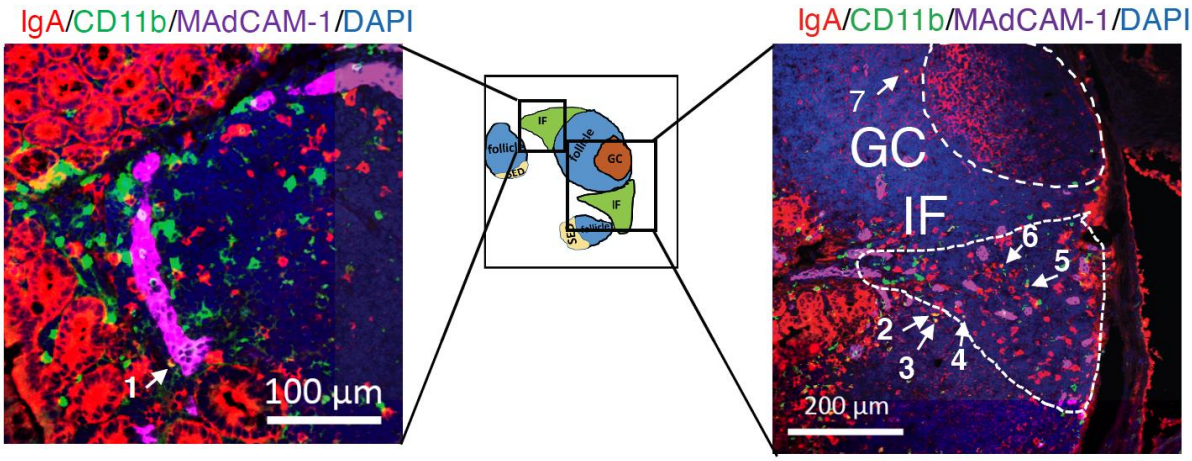

Figure 10 CD11b$^+$IgA$^+$ B cells are located in IF area.

Representative microscopy images of indicated areas showed CD11b$^+$IgA$^+$ B cells (yellow arrow, marked as 1 to 7) with staining of CD11b (green), IgA (red), MAdCAM-1 (purple) and DAPI (blue). GC and IF areas were marked by dashed white circles. Scale bar, 100 μm, 200 μm.

3-6 Transferred CD11b$^+$IgA$^+$ PP B cells entered GCs in 40 hours.

The next question is whether CD11b$^+$IgA$^+$ PP B cells subsequently migrate into the GCs from outside of GCs. We sorted CD11b$^+$IgA$^+$ and CD11b$^-$IgA$^+$ PP B cells, and then labeled and separately injected them into a PP from different IgA-Cre/YC3.60^{flox} reporter mice. Since PP GCs can be identified by the IgA$^+$ B cells-enriched area (Figure 8a), these reporter mice with YC3.60 fluorescence at IgA$^+$ cells

enable us to readily identify PP GCs. One hour after injection, the injected CD11b$^-$IgA$^+$ B cells were located inside the GCs (Figure 11), suggesting that CD11b$^-$IgA$^+$ B cells are GC B cells. In contrast, the injected CD11b$^+$IgA$^+$ B cells did not enter GCs but surrounded them (Figure 11). Forty hours after injection, the injected CD11b$^+$IgA$^+$ B cells also entered the GC (Figure 11). Thus, CD11b$^+$IgA$^+$ B cells originally located in the IF area will migrate into GCs. Thus, we thought CD11b$^+$IgA$^+$ B cells may be pre-GC B cells.

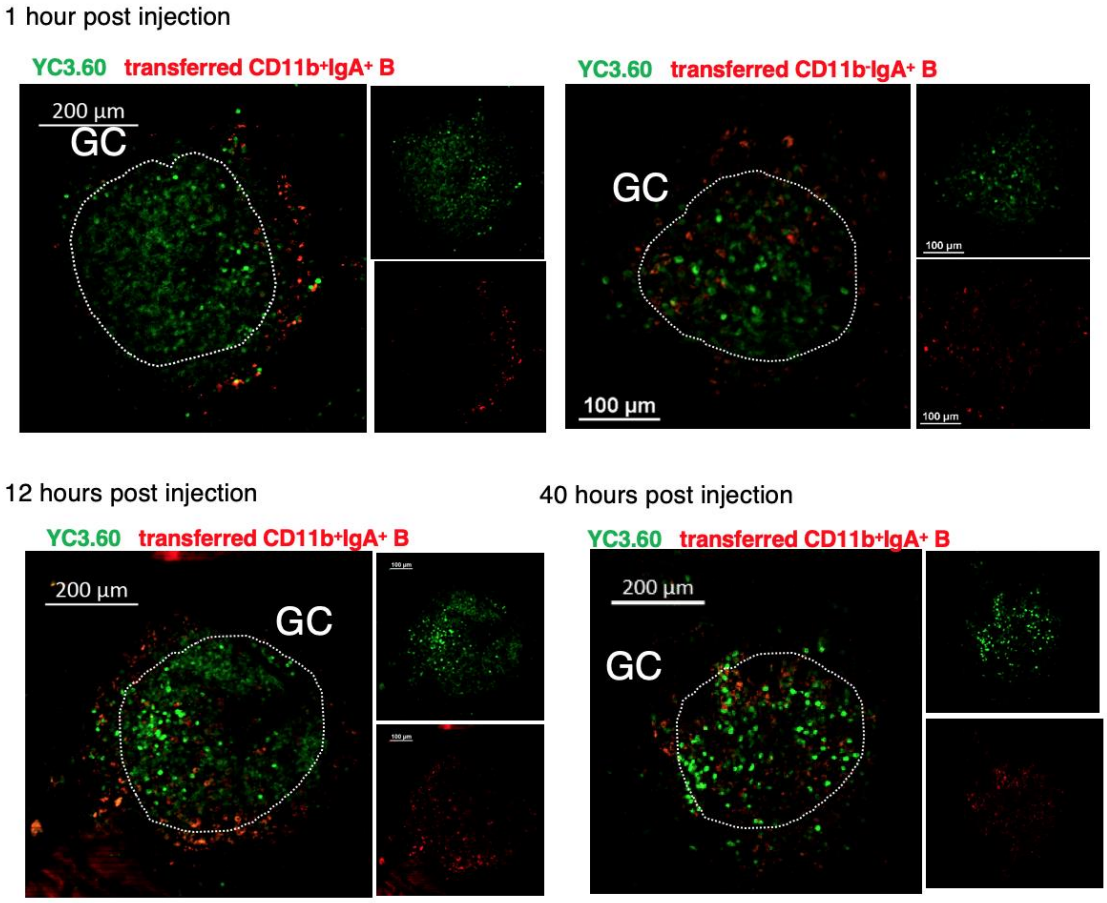

Figure 11 Transferred CD11b$^+$IgA$^+$ PP B cells entered GCs in 40 hours.

Representative images demonstrated the location of transferred CD11b$^+$IgA$^+$ PP B cells (red) or CD11b$^-$ IgA$^+$ PP B cell (red) in the PP of IgA/Cre-YC3.60 mice. CD11b$^+$IgA$^+$ PP B cells and CD11b$^-$IgA$^+$ PP B cells were directly injected into a PP of IgA/Cre-YC3.60 mice, respectively. GC boundary (dashed white line) was identified by IgA-YC3.60 (green) enriched area. Data are representative from 3 independent experiments. Scale bar, 200μm, 100 μm.

3-7 Gene expression indicates that CD11b$^+$IgA$^+$ PP B cells are pre-GC B cells.

To further confirm the pre-GC B cell phenotypes, we sorted the $CD11b^{+}IgA^{+}$ and $CD11b^{-}IgA^{+}$ PP B cells and compared their gene expression by microarray analysis (Figure 12a, b). We confirmed the gene expressions of *itgam* (CD11b) and *igha* (IgA) in $CD11b^{+}IgA^{+}$ PP B cells (Figure 12b). $CD11b^{+}IgA^{+}$ B cells expressed GC genes at relatively lower levels and non-GC genes at relatively higher levels than $CD11b^{-}IgA^{+}$ B cells, indicating that $CD11b^{+}IgA^{+}$ B cells are distinct population from $CD11b^{-}IgA^{+}$ B cells.

To confirm our microarray result, we further performed quantitative PCR (qPCR) to compare the gene expression of $CD11b^{+}IgA^{+}$ B cells with that of sorted GC ($PNA^{high}B220^{+}$) and non-GC ($PNA^{low}B220^{+}$) PP B cells (Figure 12a, c). We selected three GC genes, including *bcl6* (a main transcription factor during GC reaction)[33,34], *aicda* (an enzyme inducing both the SHM and class-switch recombination) [34-38] and *s1pr2* (a receptor regulating B cell positioning in GCs and outside GCs)[39,40]. As shown in Figure 12c, PP GC B cells highly express *bcl6*, *aicda* and *s1pr2*, while non-GC PP B cells do not express three genes. Both $CD11b^{+}IgA^{+}$ PP B cells and $CD11b^{-}IgA^{+}$ PP B cells express *bcl6*, *aicda* and *s1pr2* at similar levels as PP GC B cells (Figure 12c). We selected two non-GC genes, *gpr183* (a receptor regulating B cell position between follicle and outside follicle)[41-43] and *bcl2* (a transcription factor encoding anti-apoptotic molecule highly expressed in non-GC B cells)[44]. The expression levels of these selected genes of both $CD11b^{+}IgA^{+}$ and $CD11b^{-}IgA^{+}$ PP B cells are distinct from those of the non-GC B cells (Figure 12c), indicating both populations are likely GC B cells but not non-GC B cells.

Since pre-GC B cells upregulate *irf4*, a transcription factor which has been demonstrated to be necessary for the initiation of GC reaction[24], we further analyzed the expression of *irf4*. $CD11b^{+}IgA^{+}$ PP B cells express higher *irf4* than $CD11b^{-}IgA^{+}$ PP B cells (Figure 12c), indicating that they are pre-GC B cells.

However, considering that some GC LZ B cells also highly express *irf4*[5,8], we subsequently analyzed the CXCR4 and CD86 expressions of $CD11b^{+}IgA^{+}$ PP B cells by flow cytometry. Since GC LZ B cells are identified as $CD86^{high}CXCR4^{low}$ B cells[8,45], the lower expression of CD86 and higher expression of CXCR4 in $CD11b^{+}IgA^{+}$ B cells compared with $CD11b^{-}IgA^{+}$ B cells (Figure 12d) demonstrated that $CD11b^{+}IgA^{+}$ B cells are not GC LZ B cells, but are pre-GC B cells.

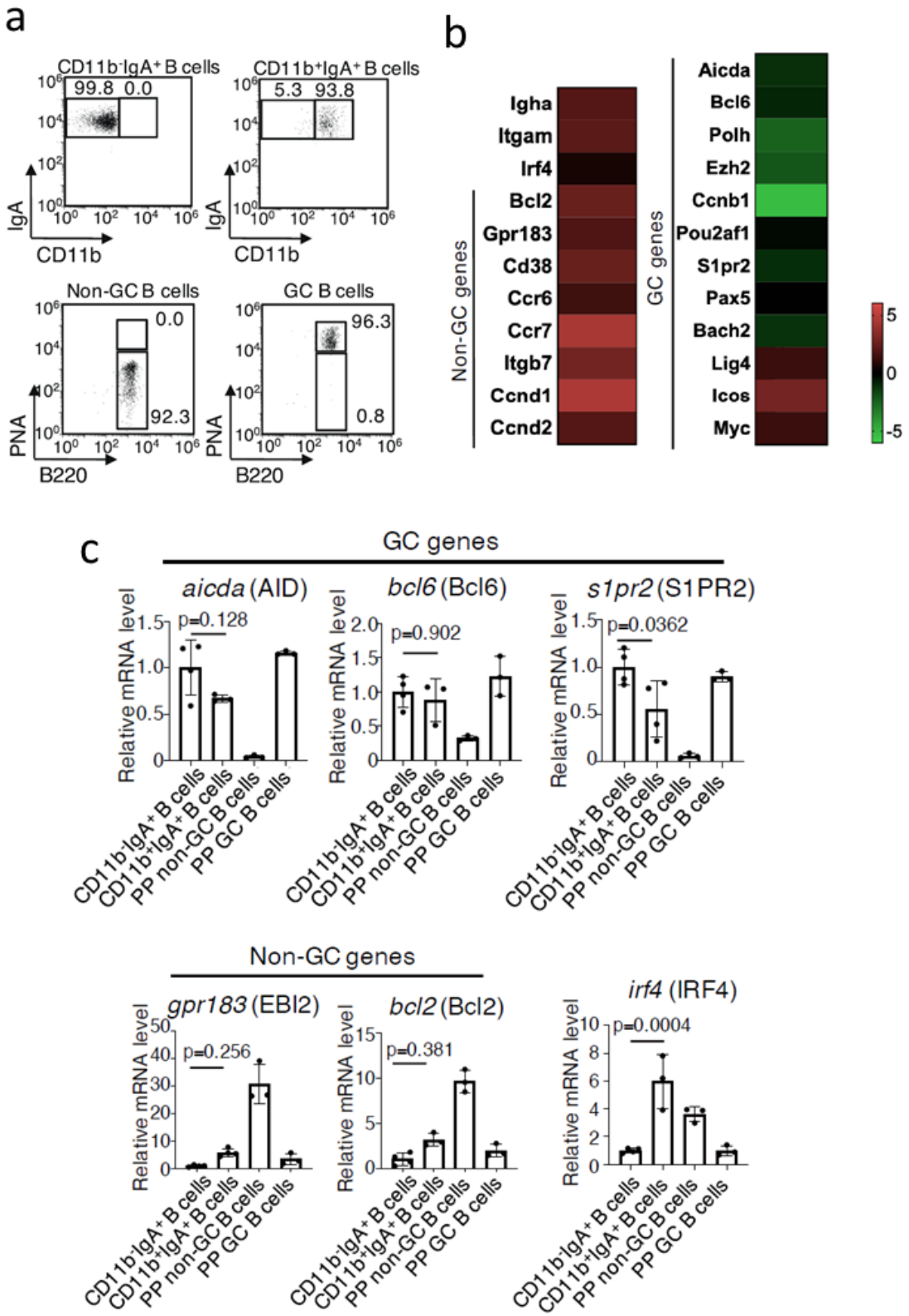
a
CD11b-IgA+ B cells
99.8 0.0
CD11b+IgA+ B cells
5.3 93.8
IgA
CD11b
Non-GC B cells
0.0
92.3
GC B cells
96.3
0.8
PNA
B220
b
Igha
Itgam
Irf4
Bcl2
Gpr183
Cd38
Ccr6
Ccr7
Itgb7
Ccnd1
Ccnd2
Non-GC genes
GC genes
Aicda
Bcl6
Polh
Ezh2
Ccnb1
Pou2af1
S1pr2
Pax5
Bach2
Lig4
Icos
Myc
5
0
-5
c
GC genes
aicda (AID)
bcl6 (Bcl6)
s1pr2 (S1PR2)
Relative mRNA level
p=0.128
p=0.902
p=0.0362
CD11b-IgA+ B cells
CD11b+IgA+ B cells
PP non-GC B cells
PP GC B cells
Non-GC genes
gpr183 (EBI2)
bcl2 (Bcl2)
irf4 (IRF4)
p=0.256
p=0.381
p=0.0004

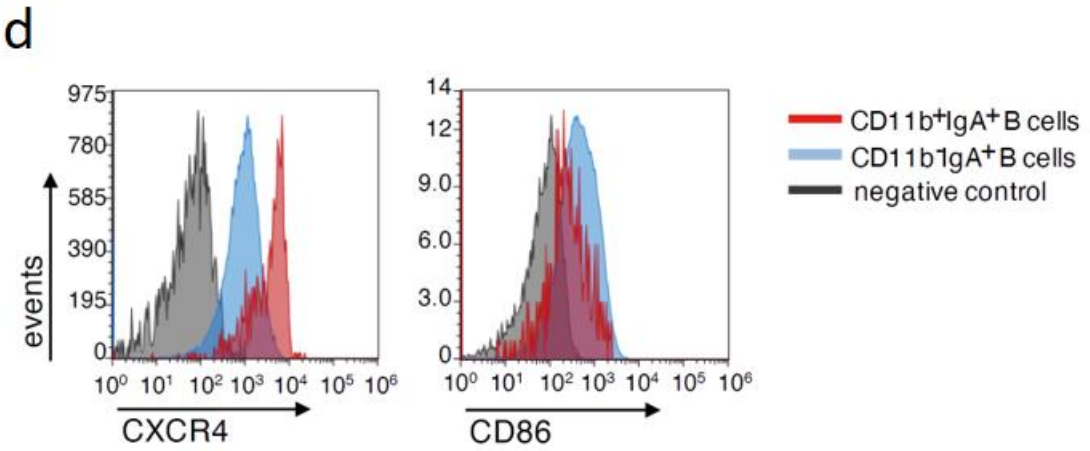

Figure 12 CD11b$^+$IgA$^+$ PP B cells express pre-GC B cell genes.

(a) CD11b$^+$IgA$^+$ PP B cells, CD11b$^-$IgA$^+$ PP B cells, PP GC B cells (PNA^{hi}B220$^+$ cells) and non-GC B cells (PNA^{lo}B220$^+$ cells) were sorted by flow cytometer. (**b)** Heatmap indicating the log fold change (CD11b$^+$IgA$^+$ B cells/ CD11b$^-$IgA$^+$ B cells) in expression of indicated genes by microarray analysis. **(c)** Expression levels of indicated GC specific genes and non-GC specific genes and pre-GC gene were analyzed by qPCR and normalized to those from *β-actin* gene. The mean of relative expression levels of CD11b$^-$IgA$^+$ B cells are taken as 1. Each spot represents the mean of technical triplicates. Bar graphs show the mean values (±SD) of three or four independent measurements. Data were analyzed by ANOVA followed by Tukey's multiple comparisons. (**d**) Flow cytometry histograms depicting expression of surface markers of CXCR4 and CD86 in CD11b$^+$IgA$^+$ B cells and CD11b$^-$IgA$^+$ B cells. Representative data are from at least five independent experiments.

3-8 CD11b$^+$IgA$^+$ PP B cells interact with CD4$^+$ T cells in IF area

To enter GCs, the pre-GC B cells must interact with T or DCs, as reported previously[4,5]. So, we checked whether CD11b$^+$IgA$^+$ PP B cells interact with CD4$^+$ T cells before entering GCs. IgA$^+$ PP B cells were not CD4$^+$ positive in singlet B cell gate by flow cytometry (Figure 13a). However, a distinct population of IgA$^+$CD4$^+$ double positive PP cells exist in the conjugated B cells (Figure 13a), indicating that these IgA$^+$ PP B cells are interacting with CD4$^+$ T cells. In particular, more than 40% of CD11b$^+$IgA$^+$ B cells showed CD4$^+$ T cell-conjugation (Figure 13b, c), suggesting that CD11b$^+$IgA$^+$ PP B cells are interacting with CD4$^+$ T cells. On the other hand, about 14.5% of CD11b$^-$IgA$^+$ PP B cells are interacting with CD4$^+$ T cells, maybe CD4$^+$ T follicular helper (T_{FH}) cells in the GC LZ (Figure 13b, c)[8].

Confocal microscopic imaging of the conjugated cells sorted from PPs further confirmed the interaction between CD11b$^+$IgA$^+$ PP B cells and CD4$^+$ T cells (Figure 13d). Thus, our results clearly indicate that CD11b$^+$IgA$^+$ PP B cells are pre-GC PP B cells.

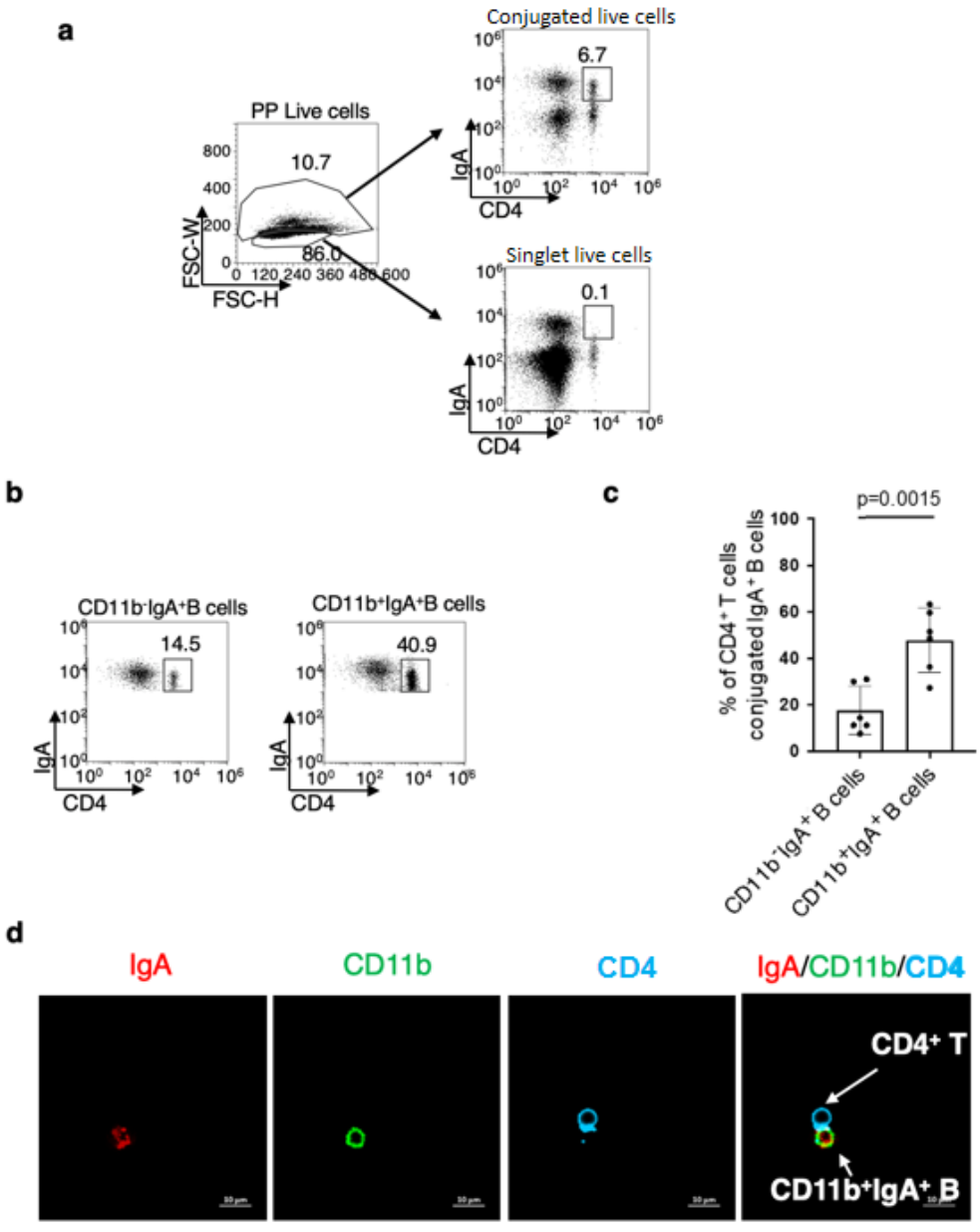

Figure 13 CD11b$^+$IgA$^+$ PP B cells interact with CD4$^+$ T cells in IF area.

(a) Representative flow cytometry analysis of singlet and conjugated IgA$^+$ B cells and CD4$^+$ T cells. (**b)** Representative flow cytometry analysis of CD11b$^-$IgA$^+$ B cells and CD11b$^+$IgA$^+$ PP B cells with CD4$^+$ T cells in conjugated gate. (**c)** Percentage of the CD4$^+$ T cells in conjugate with CD11b$^+$IgA$^+$ PP B cells and CD11b$^-$IgA$^+$ PP B cells. Bar graphs show the mean values (±SD) of six independent measurements. Data was analyzed by unpaired t test. (**d)** Representative imaging of sorted CD11b$^+$IgA$^+$ PP B cells conjugate with CD4$^+$ T cells. Scale bar, 10μm

3-9 CD11b^{+}IgA^{+} PP B cells accumulate SHM in their Ig genes

To check whether CD11b^{+}IgA^{+} B cells are derived from newly activated naïve B cells, we sequenced both the rearranged VDJ region and the downstream intronic sequences of IgH of CD11b^{+}IgA^{+} and CD11b^{-}IgA^{+} PP B cells, where SHM are introduced during GC reaction (Figure 14a, b) [13,30]. More than 80% of the sequences from CD11b^{+}IgA^{+} PP B cells (21 out of 25 clones), as well as CD11b^{-}IgA^{+} PP B cells (32 out of 39 clones), have mutations (Figure 14b), indicating that CD11b^{+}IgA^{+} PP B cells are derived not only from newly activated naïve B cells but also from memory B cells re-entering GC, as reported previously[5,7,15].

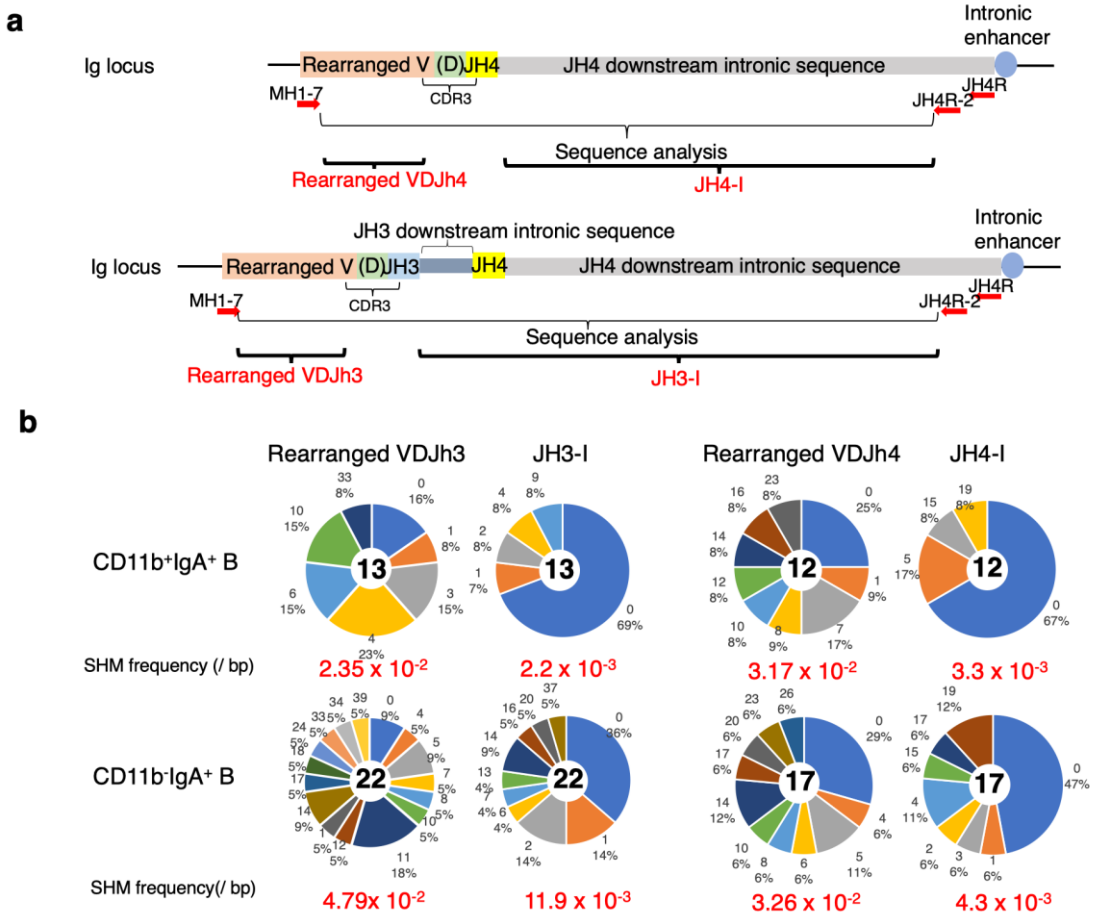

Figure 14 CD11b^{+}IgA^{+} PP B cells carry SHM.

(a) The rearranged VDJ region and downstream intronic sequences amplified by PCR were analyzed for SHM frequency. (**b)** Analysis of SHM frequency of the rearranged VDJH3 and JH3 downstream intronic sequences (JH3-I) and rearranged VDJH4 and JH4 downstream intronic sequences (JH4-I) from sorted CD11b^{-}IgA^{+} and CD11b^{+}IgA^{+} B cells from PPs of 26 WT mice. Segment sizes in pie charts are

proportional to the number of sequences with the mutation numbers observed in each clone. The numbers in the middle of the pie charts represent the numbers of analyzed clones.

3-10 Bacterial antigens induce CD11b expression of spleen B cells *in vitro*.

Our findings concerning $CD11b^{+}IgA^{+}$ PP B cells raise another question of, what triggers CD11b expression of pre-GC B cells. Besides stimulating antigens, B cells also interact with DCs and T cells to be transformed into pre-GC B cells[4,5]. To investigate which signal induces CD11b expression, we sorted the naïve spleen B cells from unimmunized mice and cultured them *in vitro* with anti-IgM for BCR crosslinking, B cell activating factor (BAFF) for interaction with DCs, anti-CD40 for interaction with T cells (Figure 15a). However, these stimulations mimicking T-B and DC-B interactions did not induce CD11b on the naïve B cells (Figure 15b-f). Next, we stimulated the naïve B cells with different Toll-like receptor (TLR) ligands, including pam3CSK4 for TLR2, poly I:C for TLR3, LPS for TLR4, flagellin for TLR5, imiquimod for TLR7 and CpG for TLR9 (Figure 15a-f). After culturing for 3 days, the number of B cells stimulated with pam3CSK4, LPS and CpG significantly increased to levels more than those stimulated with anti-IgM, anti-CD40, BAFF, poly I:C, flagellin or imiquimod (Figure 15b, c). The percentage of the $CD11b^{+}$ B cells in the B cells stimulated with pam3CSK4 and LPS were 27.6% and 8%, respectively, while those in B cells stimulated with the other stimulations was less than 5% (Figure 15d, e). It is notable that CpG did not induce CD11b expression, although it activated B cell proliferation (Figure 15b-e). We further confirmed that *itgam* (CD11b) expression in the B cells increased only when stimulated with pam3CSK4 or LPS that are known as bacterial antigens (Figure 15f).

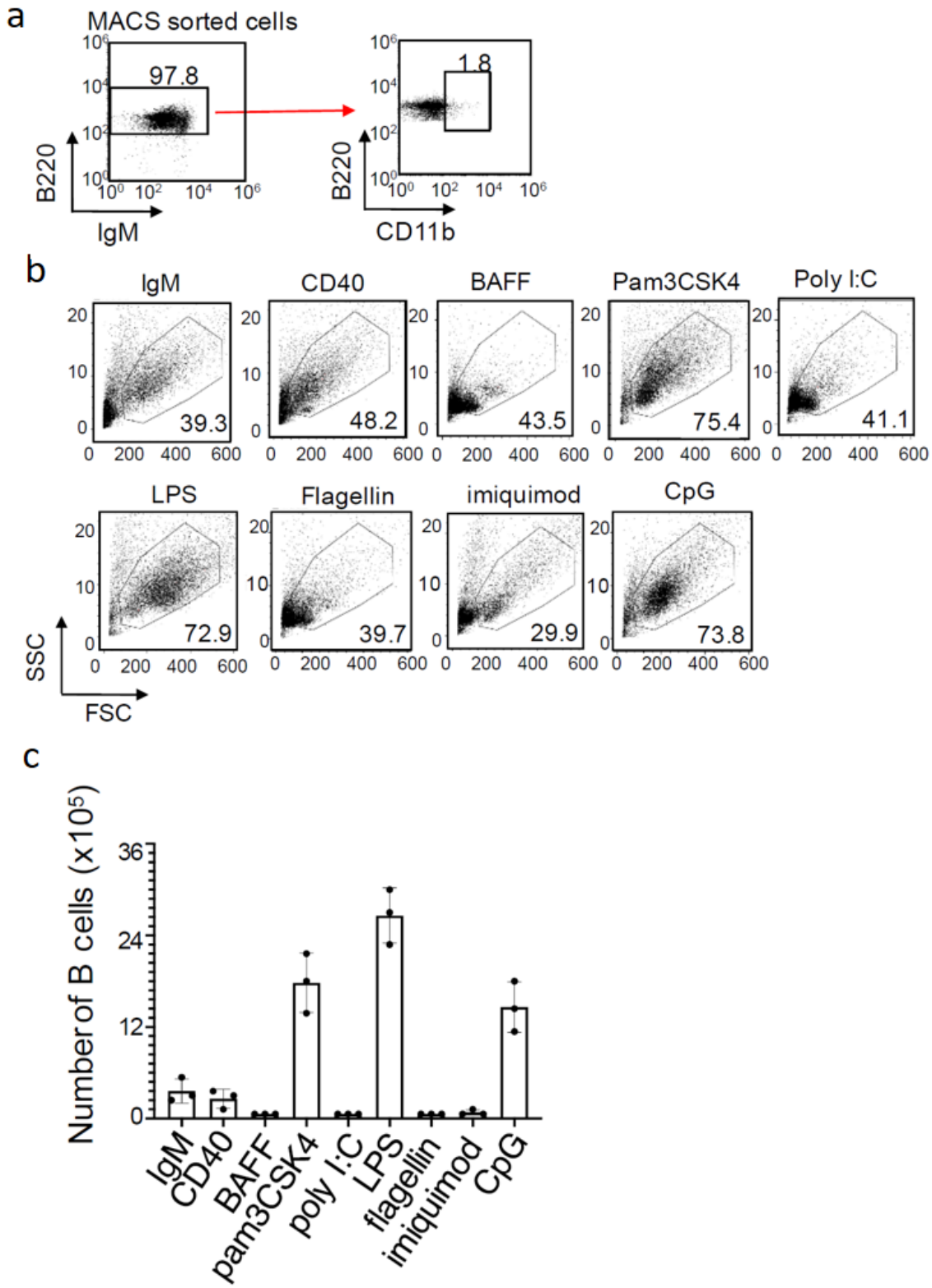
a
MACS sorted cells
97.8
1.8
B220
IgM
CD11b
b
IgM
CD40
BAFF
Pam3CSK4
Poly I:C
39.3
48.2
43.5
75.4
41.1
LPS
Flagellin
imiquimod
CpG
72.9
39.7
29.9
73.8
SSC
FSC
c
Number of B cells (x10^5)
IgM
CD40
BAFF
pam3CSK4
poly I:C
LPS
flagellin
imiquimod
CpG

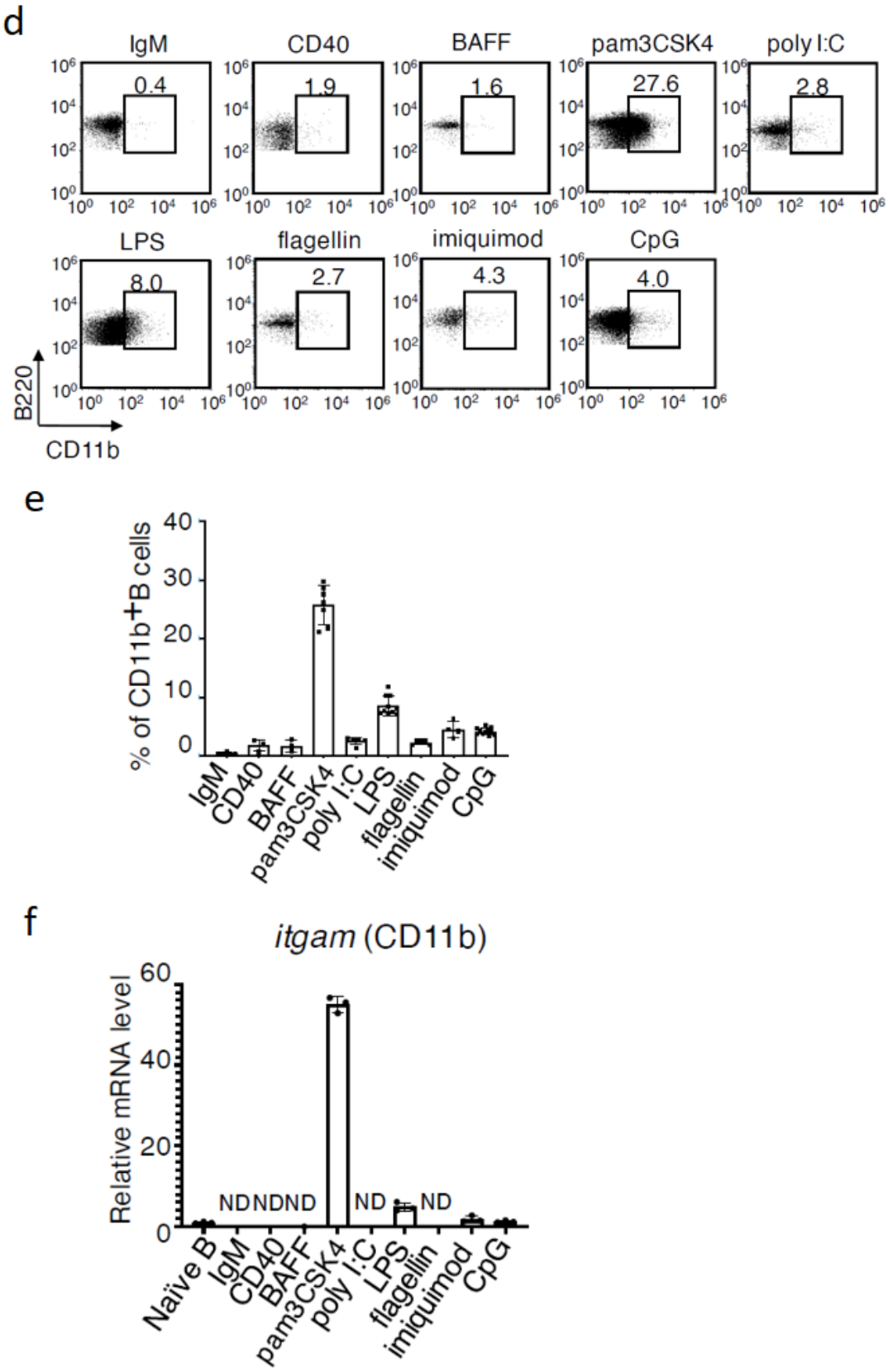

Figure 15 TLR ligand-stimulation induce CD11b expression on naïve spleen B cells.

(a) The purity of sorted naïve spleen B cells and their CD11b expression. **(b)** Lymphocyte gate of the 3-day cultured spleen naïve B cells with indicated stimulations. (**c**) Absolute numbers of the cultured spleen naïve B cells with indicated single stimulations. **(d)** Flow cytometry analysis of the CD11b expression of the indicated stimulated B cells. (**e)** Percentage of $CD11b^+$ B cells of each stimulation are shown (n=3~7). (**f)** qPCR analysis of *itgam* (CD11b) expression was performed with the sorted B cells from indicated stimulation for 3 days. (**c, e, f**) Each spot represents independent analysis. Bar graphs show the mean values (±SD) of three to seven independent measurements. ND, not detected.

3-11 Heat-killed *E. coli* induce CD11b expression on spleen B cells.

Since TLR2 and TLR4 are sensors for bacterial antigens, we then prepared heat-killed *E. coli*, which is a strong stimulant for both TLR2 and (or) TLR4[46,47], and found that heat-killed *E. coli* significantly induced CD11b expression on spleen B cells (Figure 16). These results showed that the bacterial antigens, TLR2 and TLR4 ligands, induced CD11b on B cells.

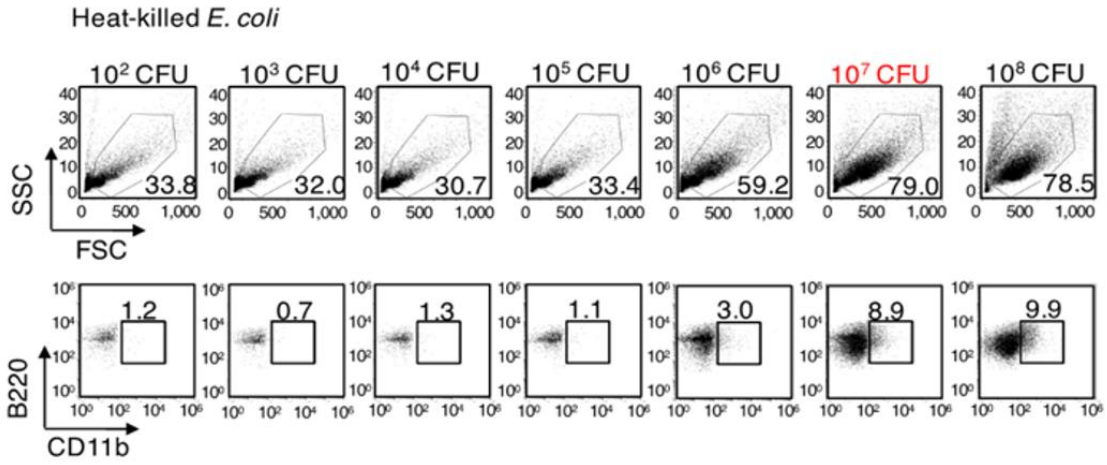

Figure 16 Heat-killed *E. coli* induced CD11b expression on naïve spleen B cells.
Flow cytometry analysis of the lymphocyte gate (up) and CD11b expression (down) of the heat-killed *E. coli* stimulated B cells for 3 days. The CFU number above indicated the amount of heat-killed *E. coli* in 1 ml medium. Selected conditions for replicated experiments are marked in red color.

3-12 $CD11b^+$ B cells lost their CD11b expression by T-B and DC-B interaction.

Since the B cells inside PP GCs do not express CD11b (Figure 8a), we hypothesized that CD11b expression on B cells may be transient and convertible via T-B or DC-B interaction. To follow

the surface phenotypes, we utilized an *in vitro* induced GC B cell (iGB) culture system that mimics the role of T and DC cells for inducing GC-like B cells on the feeder layer of 40LB cells expressing CD40L and BAFF[29]. After the cell culture with iGB system, the sorted $CD11b^{+}IgA^{+}$ PP B cells can proliferate at similar levels as the sorted $CD11b^{-}IgA^{+}$ PP B cells or naïve spleen B cells (Figure 17a). Indeed, the sorted $CD11b^{+}IgA^{+}$ PP B cells lost their CD11b expression after one day culture with the iGB system (Figure 17b). Similarly, the pam3CSK4-induced $CD11b^{+}$ spleen B cells lost the CD11b expression after culturing with the iGB system for 4 days (Figure 17c).

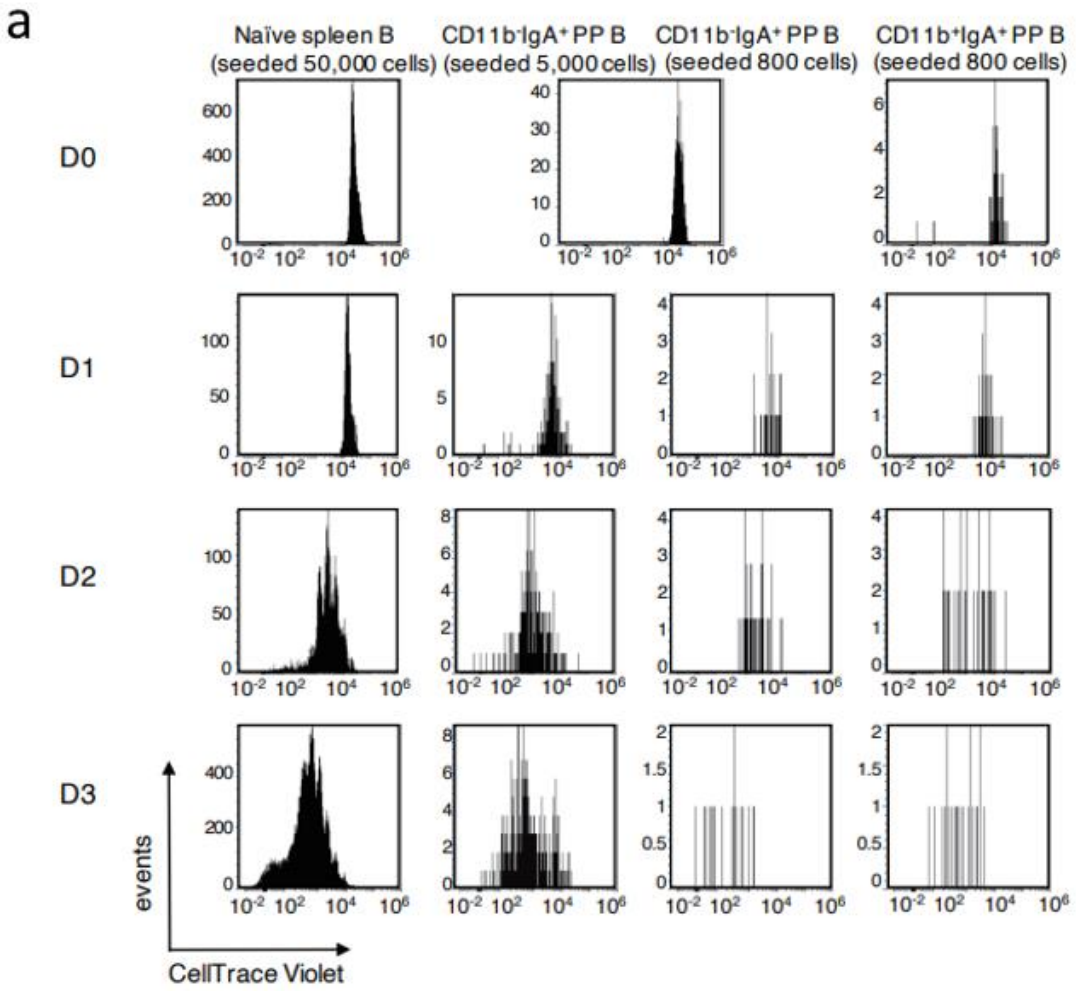
a
Naïve spleen B (seeded 50,000 cells)
CD11b-IgA+ PP B (seeded 5,000 cells)
CD11b-IgA+ PP B (seeded 800 cells)
CD11b+IgA+ PP B (seeded 800 cells)
D0
D1
D2
D3
events
CellTrace Violet

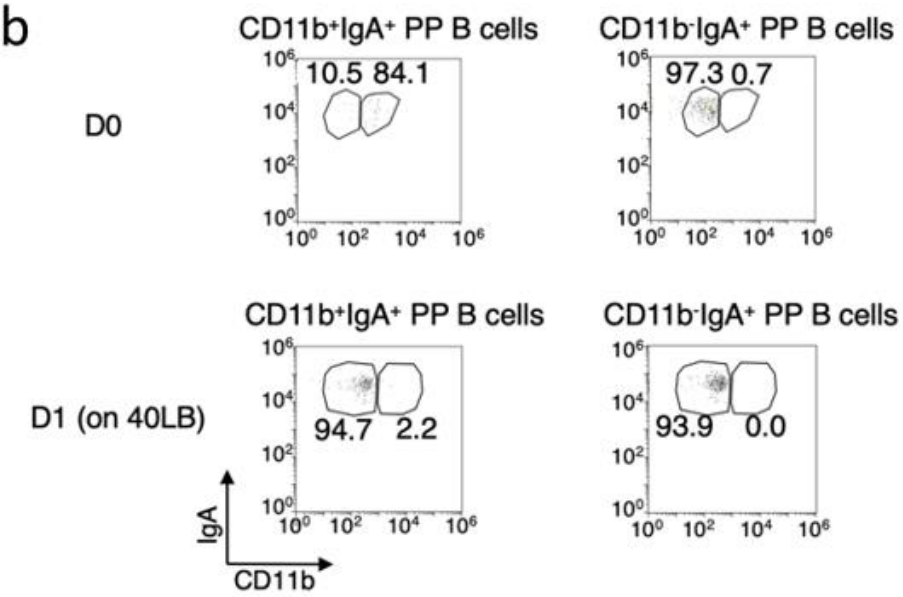
b
CD11b+IgA+ PP B cells
CD11b-IgA+ PP B cells
D0
10.5 84.1
97.3 0.7
D1 (on 40LB)
94.7 2.2
93.9 0.0
IgA
CD11b

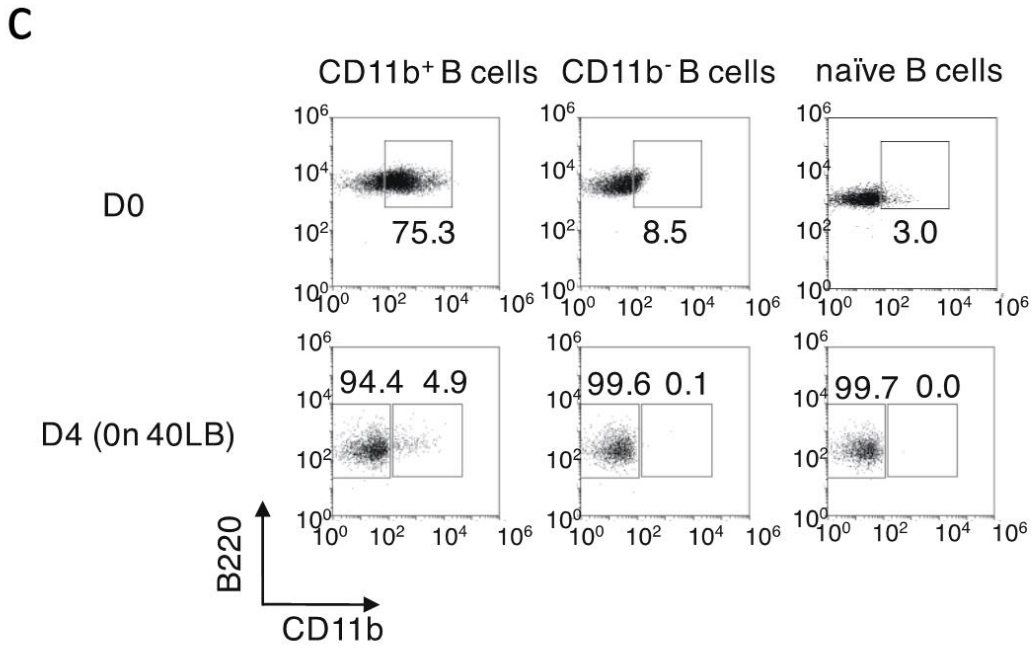

Figure 17 CD11b$^+$ B cell lost CD11b expression on 40LB cells.

(**a**) Naïve spleen B cells, sorted CD11b$^+$IgA$^+$ PP B cells and CD11b$^-$IgA$^+$ PP B cells labeled with CellTrace Violet were cultured for 3 days on 40LB system with IL-21 or IL-4 stimulation. About 50,000 naïve Spleen B cells and 5,000 sorted CD11b$^-$IgA$^+$ B cells were prepared as positive control. Eight-hundred sorted CD11b$^+$IgA$^+$ PP B cells and CD11b$^-$IgA$^+$ PP B cells were prepared to monitor their proliferation. Representative data are shown from two independent experiments. **(b)** CD11b expression was analyzed by flow cytometry on day 0 and day 1. (**c**) Spleen naïve B cells were cultured with pam3CSK4-stimulation for 3 days to induce CD11b$^+$ B cells. About 1.5 x 10^5 sorted pam3CSK4 induced CD11b$^+$ spleen B cells and CD11b$^-$ spleen B cells were seeded on 40LB cells with 1 ng/ml IL-4. Negatively sorted spleen naïve B cells were used to as control. The CD11b expression of indicated B cells seeded on 40LB system were analyzed on D0 and D4. Representative data are shown from three independent experiments.

3-13 The pam3CSK4-induced CD11b$^+$ B cells downregulate their CD11b expression with the treatment of soluble anti-CD40 Ab and anti-IgM Ab.

To analyze whether BCR-crosslinking, anti-CD40 Ab or soluble BAFF downregulate CD11b expression, we stimulated the spleen naïve B cells with anti-IgM Ab, anti-CD40 Ab and (or) BAFF in addition to pam3CSK4 (Figure 18a). Spleen naïve B cells treated with anti-CD40 Ab and anti-IgM Ab

significantly suppressed CD11b expression, even in the presence of pam3CSK4 (Figure 18a-c) indicating that T-B cell interaction and BCR-crosslinking downregulate the CD11b expression on B cells. Therefore, it is reasonable that we found quite a few $CD11b^{+}IgA^{+}$ PP B cells *in vivo* (Figure 6).

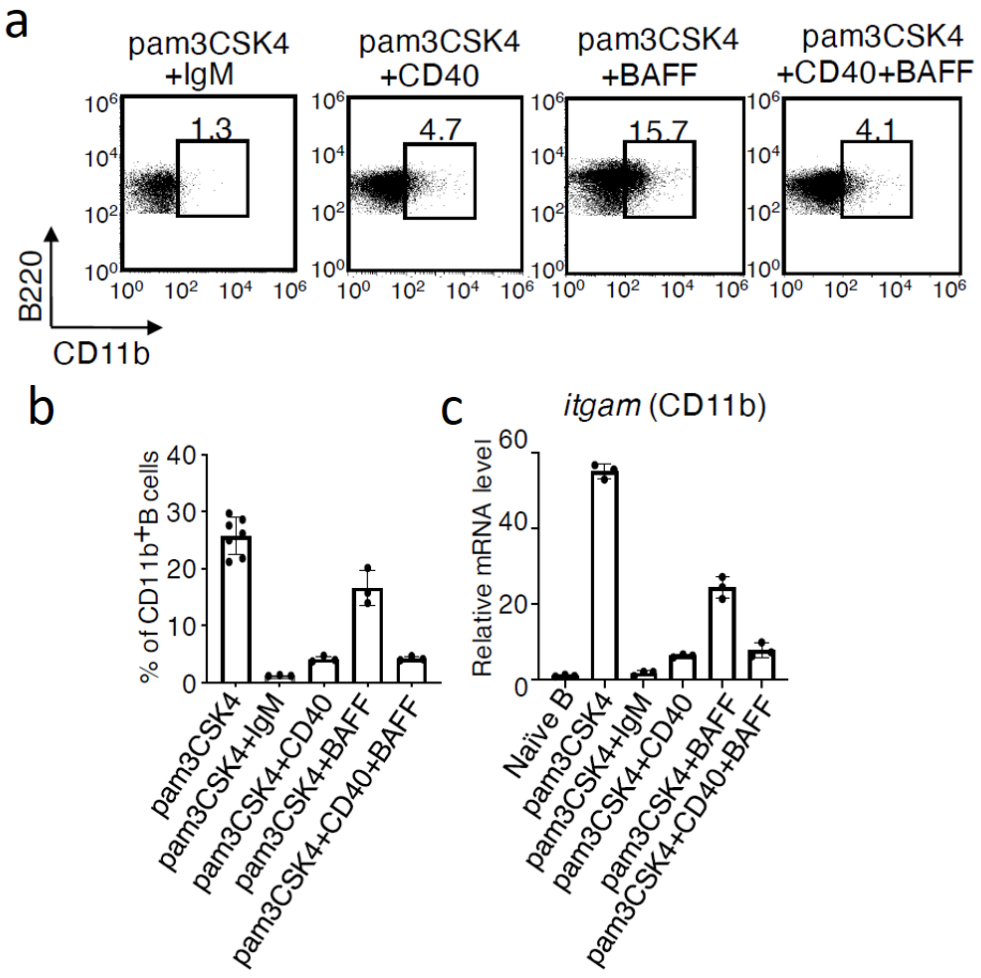

Figure 18 CD40 stimulation suppresses bacterial antigen-induced CD11b expression on naïve spleen B cells.

(**a)** Spleen naïve B cells with indicated stimulations were cultured *in vitro* for three days. Flow cytometry analysis of the CD11b expression of the stimulated B cells. (**b**) Percentage of $CD11b^{+}$ B cells of each stimulation are shown (*n*=3~7). (**c)** qPCR analysis of *itgam* (CD11b) expression was performed with the sorted B cells from indicated stimulation for 3 days. (**b, c**) Data of Pam3CSK4-stimulated spleen B cells are from Figure 13. Each spot represents independent analysis. Bar graphs show the mean values (±SD) of three to seven independent measurements. (**a**) Representative data are shown from at least three independent experiments.

3-14 CD11b expression is induced by some unknown NOD2-mediated stimuli derived from bacteria.

To further confirm whether TLR2 and TLR4 play a role in the induction of CD11b expression of spleen B cells, we stimulated spleen B cells with pam3CSK4, LPS, CpG, and heat-killed *E. coli* in the presence of TLR1/2 inhibitor, TLR4 inhibitor or NOD2 inhibitor. NOD2 is known to mediate in the downstream signaling of TLR2[48]. Interestingly, with TLR1/2 inhibitor, pam3CSK4 and heat-killed *E. coli* increased the percentages of $CD11b^+$ B cells, while TLR4 inhibitor did not (Figure 19a). On the other hand, NOD2 inhibitor strongly suppressed CD11b expression on B cells stimulated with pam3CSK4 and heat-killed *E. coli* (Figure 19a), although muramyl dipeptide (MDP), the ligand of NOD2, did not induce CD11b expression (Figure 19b). This observation strongly suggests that CD11b expression is not directly induced by TLR2 or TLR4 activation, but partly by NOD2-mediated stimuli derived from bacteria (Figure 19a).

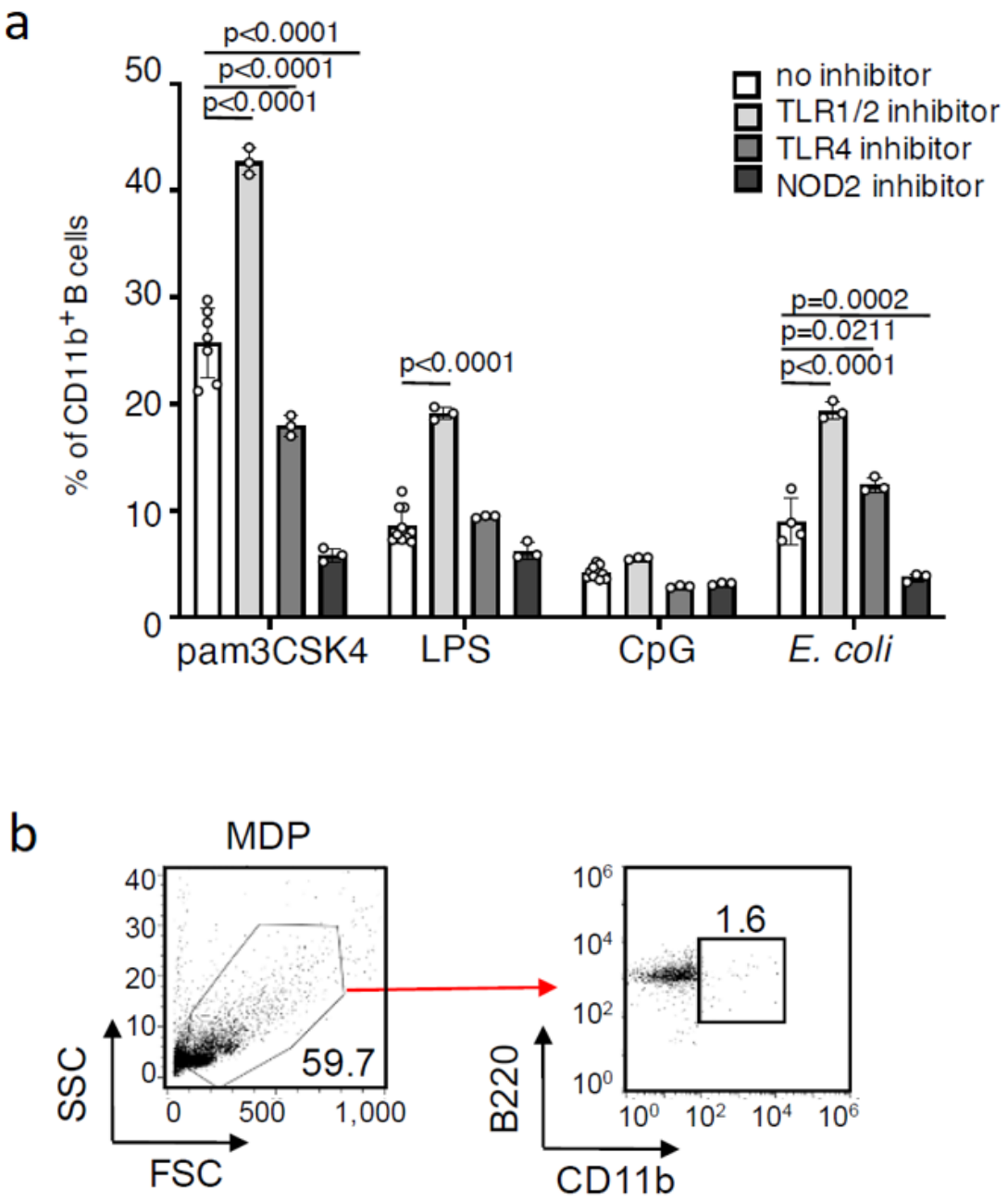

Figure 19 NOD2 regulates CD11b expression on B cells.

(a) Percentages of $CD11b^+$ B cells of each stimulation with indicated inhibitors. Data were analyzed by two-way ANOVA followed by Tukey's multiple comparisons. (**b**) Lymphocyte gate and CD11b expression of the cultured spleen naïve B cells with MDP. Representative data are from three independent experiments.

3-15 CD11b expression is induced by harmful bacteria.

The next question is what kind of bacteria can induce pre-GC B cells through CD11b expression. We selected *E. coli* and *S. enterica* as harmful bacteria, and *Bifidobacterium bifidum* (*B. bifidum*) and *B. breve* as representative beneficial bacteria. By *in vitro* stimulation, *E. coli* and *S. enterica* induced expression of CD11b on B cells, while *B. bifidum* and *B. breve* did not (Figure 16 and 20).

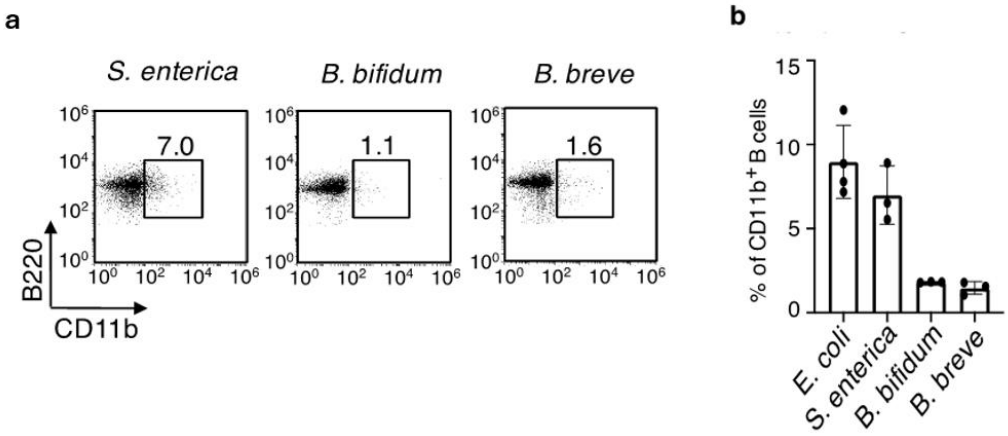

Figure 20 Heat-killed harmful bacteria induced CD11b expression on naïve spleen B cells.
(a) Flow cytometry analysis of CD11b expression of the indicated heat-killed bacteria stimulated B cells for 3 days. (b) Percentages of $CD11b^+$ B cells of each stimulation with indicated inhibitors. Bar graphs show the mean values (±SD) of at least three independent measurements.

3-16 Oral administered heat-killed CD11b-inducible bacteria enhanced GC reaction *in vivo*.

Next, we checked whether those CD11b-inducible bacteria can enhance the GC reaction *in vivo*? After oral administration of pam3CSK4 or heat-killed bacteria to mice, the numbers and percentages of PP GC B cells increased in mice administered with pam3CSK4, *E. coli* and *S. enterica* in two days (Figure 21a-c), suggesting that only harmful bacteria are capable of enhancing the ongoing GC reaction *in vivo*.

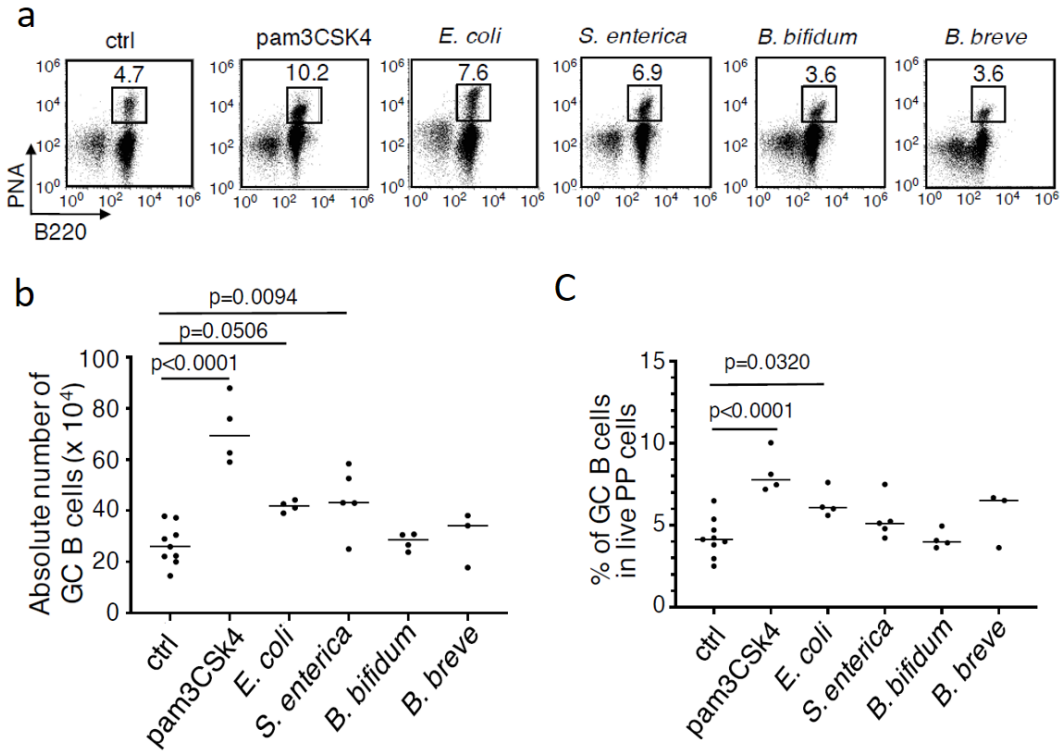

Figure 21 Oral administered CD11b-inducible bacteria enhanced the GC reaction *in vivo*.
Balb/c mice were orally administered with indicated heat-killed bacteria, pam3CSK4 or PBS (control). Two days later, flow cytometry data (**a**) of $PNA^{hi}B220^{+}$ GC B cells, absolute numbers (**b**) and percentages (**c**) of PNA^{high} $B220^{+}$ PP GC B cells from each mouse were calculated. Data were analyzed by one-way ANOVA followed by Tukey's multiple comparisons.

3-17 CD11b transient expression enables cultured B cells to enter GCs

Then, we checked whether *in vitro*-induced $CD11b^{+}$ B cells can enter the existing GCs. To induce GC B cells *in vitro*, we stimulated the spleen naïve B cells with pam3CSK4 or heat-killed *E. coli in vitro* to induce CD11b, and subsequently cultured them on 40LB cells for 4 days. Notably, most of the iGB cells pre-stimulated with pam3CSK4 or heat-killed *E. coli* for CD11b expression entered GC after intravenous injection to mice, while iGB cells without CD11b-inducible bacterial antigen stimulation, such as CpG and anti-IgM, did not enter GC (Figure 22).

Taken together, our results show that CD11b expression on B cells before T-B or DC-B interaction is essential for pre-GC B cells to enter GCs, which is consistent with a previous report that bacterial antigens, as non-self antigens, are important to evoke GC reaction[49].

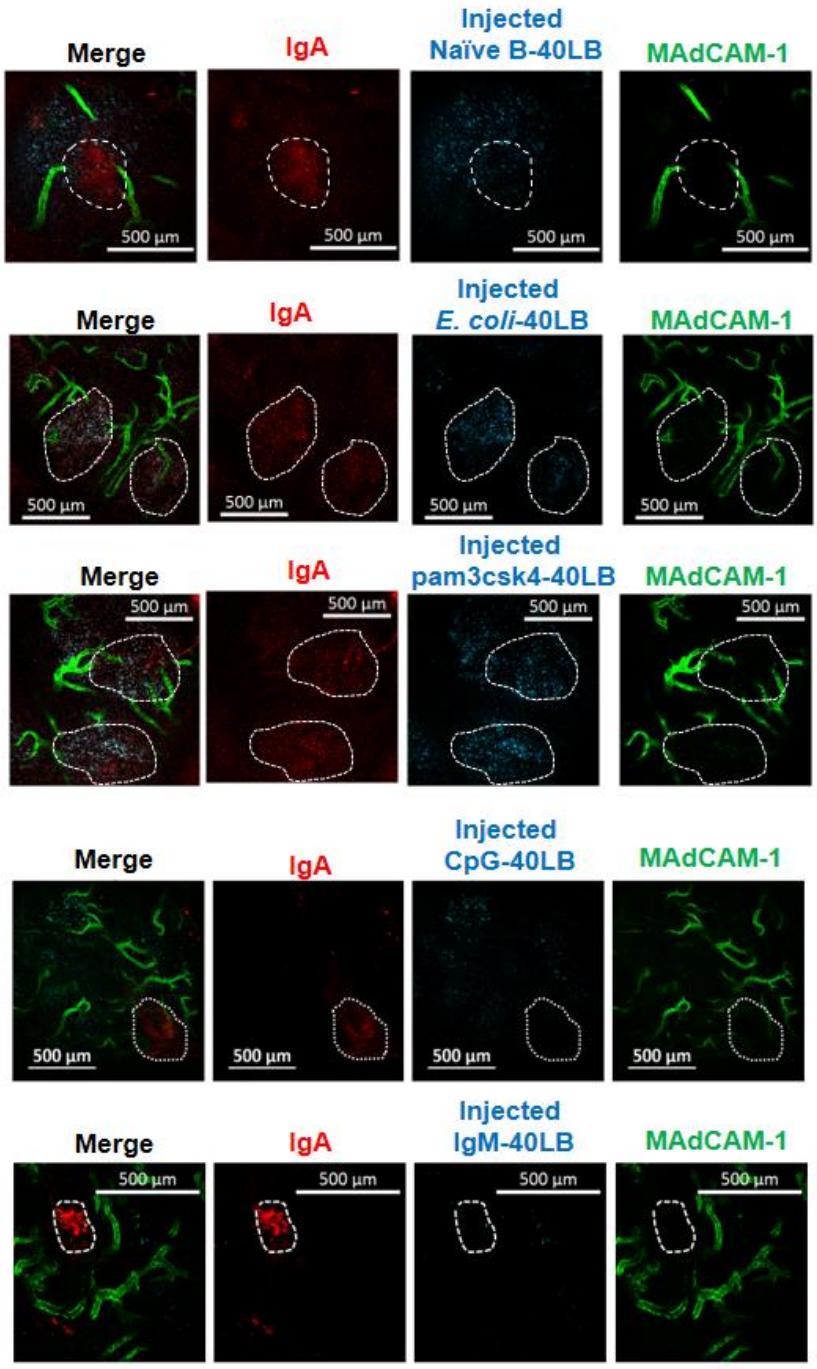

Figure 22 Intravenously injected iGB cells pre-stimulated with bacterial antigen entered PP GCs. Indicated iGB cells were sorted, labeled (cyan) and then intravenously injected to mice, independently. Scale bar, 500 μm. GC was indicated by dashed circle.

3-18 CD11b-inducible heat-killed bacteria function as effective mucosal adjuvant and induce antigen-specific mucosal IgA

We note that TLR2 or TLR9 ligand-based adjuvants are already widely used for vaccination, since they stimulate DCs efficiently[22,50]. However, our results demonstrate that B cells can determine their own cell fate to pre-GC B cells before receiving help from DC and T cells (Figure 22). Therefore, we hypothesized that pam3cCSK4 and heat-killed *E. coli* can work as mucosal vaccine adjuvants. We orally administered mice with ovalbumin (OVA) as an antigen plus pam3CSK4 or heat-killed *E. coli* as adjuvants (Figure 23). As we expected, mice administered simultaneously with OVA plus heat-killed *E. coli* or pam3CSK4 increased OVA-specific IgA in their feces, but those administered with OVA only did not (Figure 23). Thus, our study revealed that the pre-GC surface marker, CD11b, on B cells is a promising marker for selecting an effective mucosal vaccine adjuvant, especially to enhance GC-derived high-affinity mucosal IgA.

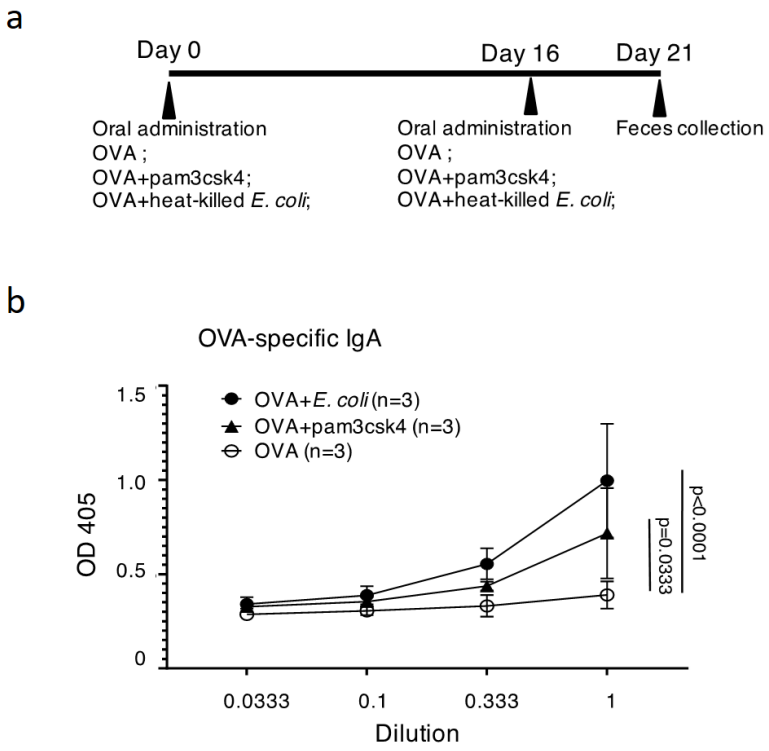

Figure 23 Oral administration of heat-killed *E. coli* enhanced mucosal OVA-specific IgA response. (a) Schedule for oral immunization. (b) Feces OVA-specific IgA after immunization. Data were analyzed by two-way ANOVA followed by Tukey's multiple comparisons.

Chapter 4 Discussion

In this study, by investigation of a distinct population of $CD11b^{+}IgA^{+}$ PP B cells, we show that CD11b is a novel surface marker of pre-GC IgA^{+} B cells in murine PPs. CD11b induction on B cells is dependent on harmful bacterial antigen stimulation but independent of activated DCs. Mice orally administered with those CD11b-inducible bacterial antigens showed enhanced mucosal antigen-specific IgA response *in vivo*. Our results demonstrate that transient CD11b expression on activated B cells before entering GC is an important step to select activated B cells appropriate for GC response.

What is the function of CD11b on B cells? Yan's group has shown that CD11b is critical in regulating BCR signaling via the Lyn-CD22-SHP-1 negative feedback pathway[18]. $CD11b^{-/-}$ mice exhibited enhanced antibody production and GC response with autoreactive B cells[19]. Accordingly, the human genetic mutations in the *ITGAM* gene (encoding CD11b) are reported as a high-risk factor of developing the autoimmune disease, such as SLE[20]. In our study, we identified CD11b expression as pre-GC B cells marker for entering GCs. Probably, CD11b transient expression is sufficient, but not necessary, for entering GCs. Once B cells are activated by bacterial stimuli, they express CD11b to avoid their hyperproliferation and production of potential autoreactive antibodies (Figure 24). In other words, CD11b expression may be critical to protecting uncontrolled GC B cell response. Subsequently, B cells begin to interact with T cells in the IF area. After T-B interaction, activated B cells lose their CD11b expression, enter GC DZ and proliferate fast and undergo SHM for obtaining high affinities (Figure 24). We propose that CD11b plays a key role in controlling the activated B cells for undergoing beneficial GC reaction but not for a harmful autoreactive response. Elucidation of precise selection mechanisms requires further investigation.

What is the deeper mechanism of CD11b regulating GC reaction? As reported previously, CD11b and CD22 form CD11b-CD22 receptor complex on B cell surface for negative regulation of BCR signaling[18]. However, the study about CD22 knockout mice showed that these mice did not exhibit GC B cell hyperactivation[51]. Because CD22-CD11b interaction is under debate, CD11b may negatively regulate BCR signaling with other surface molecules (Figure 25).

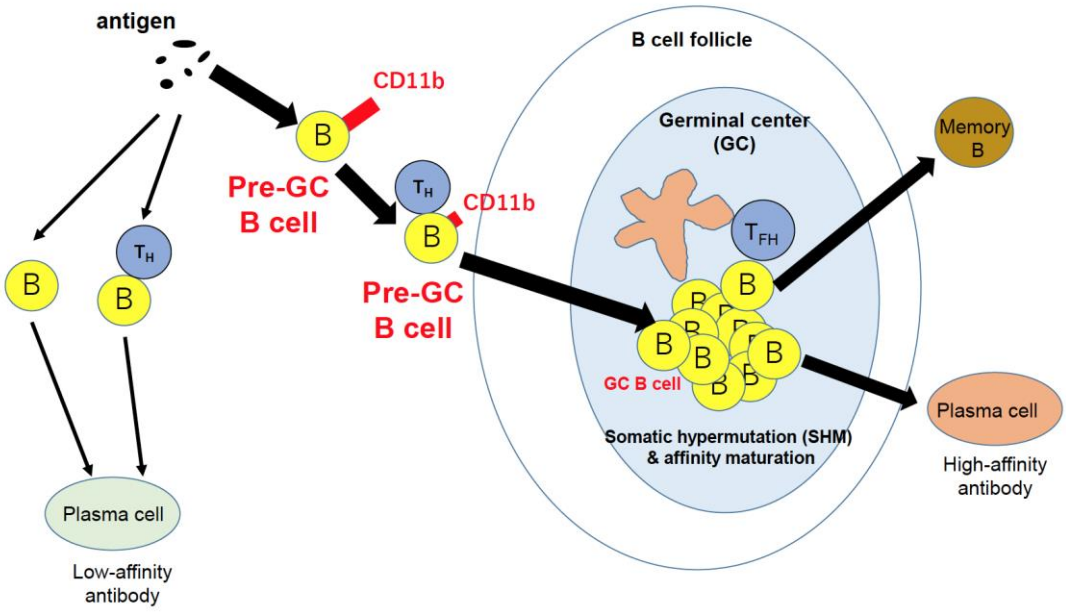

Figure 24 Transient expression of CD11b on activated pre-GC B cells

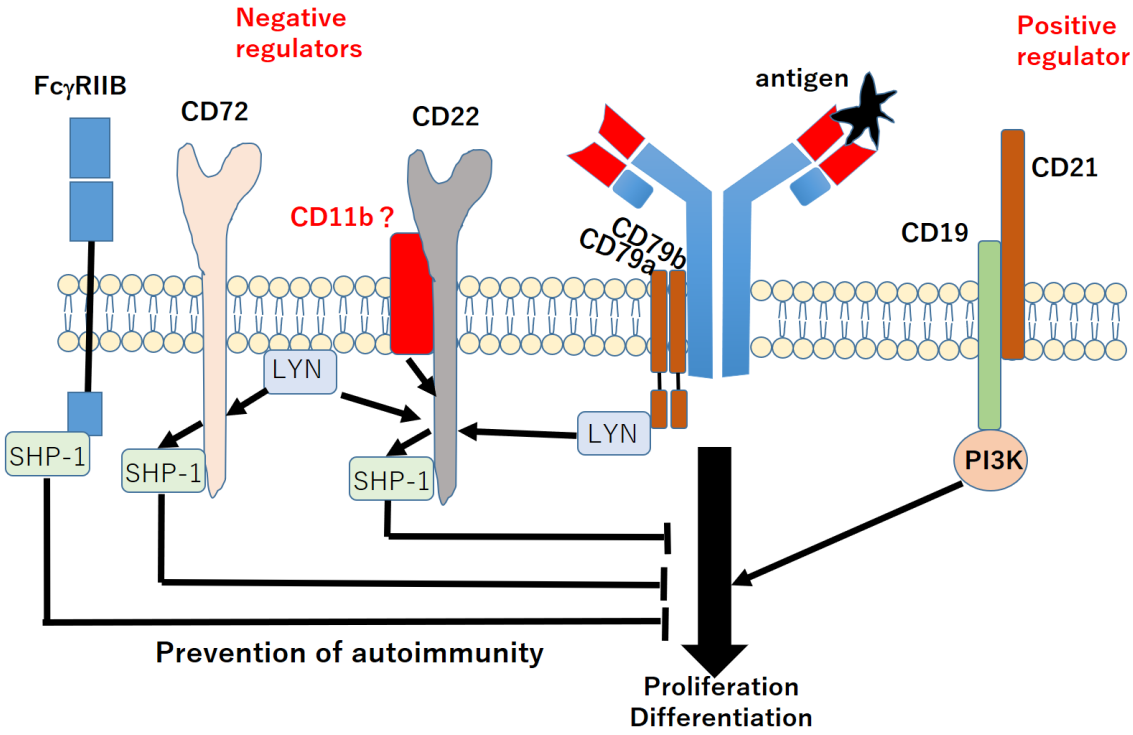

Figure 25 CD11b negatively regulates BCR signaling

Do human B cells also express CD11b by microbial antigens? Dutra's group has demonstrated that the stimulation with *Trypanosoma cruzi*-derived protein-enrich fraction leads to a higher frequency of $CD11b^+$ B cells in the patients of Chagas disease [52]. However, whether the CD11b expression in human is associated with the GC reaction remains unknown.

In order to exclude the invading harmful pathogens, the immune system has to recognize them first. We also addressed the question: which signal induces CD11b expression on B cells. Pattern recognition receptors (PRRs), such as TLRs, play a crucial role in detecting potential harmful pathogens derived from various microbes. Indeed, cell surface TLRs, including TLR1, TLR2, TLR4, TLR5 and TLR6, recognize lipids, lipoproteins or some other microbial membrane components. Intracellular TLRs, such as TLR3, TLR7 and TLR9, recognize bacteria and virus-derived nucleic acids. At first, we expected that CD11b is induced by TLR2 stimulation, since pam3CSK4, a TLR2 ligand, and heat-killed *E. coli*, strongly induced CD11b on B cells *in vitro*. *E. coli* have peptidoglycan (PGN) as a component of the bacterial cell wall, a TLR2 ligand [48]. Gram-positive bacteria contain more PGN than gram-negative bacteria. In our study, the gram-positive *Bifidobacterium* did not induce B cell proliferation or CD11b expression *in vitro*, indicating that PGN is not efficient enough to induce CD11b expression on B cells. Perhaps only specific materials derived from bacteria are the stimuli for CD11b expression. Unexpectedly pam3CSK4 plus TLR1/2 inhibitor enhanced CD11b expression on B cells. We consider that inhibitor may not work specific to TLR1/2. Also, TLR4 inhibitor did not influence the CD11b expression induced by LPS (Figure 19). This result led me to suspect that TLR4 signaling may not be involved in the induction of CD11b expression. Therefore, $TLR4^{-/-}$ and $TLR2^{-/-}$ B cells are necessary to be investigated for further study.

NOD2 is known to activate NF-κB pathway[48, 53]. MDP, a bacterial cell wall component derived from degraded PGN of both gram-positive and gram-negative bacteria, is widely used for NOD2 stimulation experimentally. Although MDP did not induce B cell proliferation or CD11b expression in our study, NOD2 inhibitor strongly suppressed the CD11b expression induced by pam3CSK4 and heat-killed *E. coli*, suggesting NOD2-mediated CD11b regulation (Figure 19). We assume that there may be additional ligands for NOD2 but MDP, which may stimulate the B cells to express CD11b. On the other hand, our results partly agree with a previous study that NOD2 can work as a negative regulator of TLR2[48]. In addition, NOD2 helps mediate the immune tolerance and homeostasis by inhibiting TLR2/4-mediated induction of inflammatory cytokine production, which is strongly associated with Crohn's disease (CD)[53]. Thus, our data suggest one possibility that TLR2-NOD2 pathway may regulate not only

inflammatory response but also GC reaction through CD11b regulation. The other study, however, has demonstrated that TLR1/2 signaling pathway is independent of NOD2[54]. Taken together with enhanced CD11b induction by TLR2 inhibitor, there is still controversy to be solved.

The investigation about the TLR and NOD2 ligands for CD11b expression has aroused another question. Which material exactly induces CD11b expression on B cells? In terms of CD11b-inducible bacterial stimuli, we have shown that *S. enterica* (gram-negative) and *E. coli* (gram-negative) as examples of harmful bacteria induce CD11b expression *in vitro* and enhance the GC reaction *in vivo*, while beneficial *Bifidobacterium* (gram-positive) species do not. We hypothesized that CD11b expression on B cells may be induced by gram-negative harmful bacteria. In our ongoing study, we prepare several different kinds of bacteria for *in vitro* stimulation to validate this question. Gram-negative *Bacteroides vulgatus* and *Klebsiella pneumonia*, as representative harmful bacteria, induce B cell proliferation and CD11b expression *in vitro*, while gram-negative *Bacteroides fragilis* only induce B cell proliferation but does not induce CD11b expression, since it is though to be beneficial to the host[55]. As we hypothesized, gram-positive *Lacticaseibacillus casei* (beneficial), *Clostridium difficile* (harmful) and *Enterococcus faecium* (harmful) did not induce CD11b expression on B cells *in vitro*. Through the CD11b expression, the immune system can distinguish the components of gram-negative harmful bacteria from those of beneficial or gram-positive bacteria is still not fully investigated. Although we cannot exactly answer what is the exact stimuli for CD11b expression and how CD11b expression helps regulate the microbe, we expect the exploration of CD11b-inducible stimuli may help us understand the immune system recognition and regulation of the microbes.

In addition to murine PP B cells, CD11b is widely expressed by the B1-B cells in murine peritoneal cavity (PerC), where the B cells are activated through a T-cell independent manner[17]. Perhaps due to lack of T-B interaction, CD11b expression on B1-B cells is not downregulated, since we demonstrated that CD40-stimulation suppresses the CD11b expression on B cells. In our current study, we have not compared the $CD11b^+$ pre-GC B cells and B1-B cells. To check whether the $CD11b^+$ B1-B cells can enter GC or not, a further investigation should be performed.

In order to develop an effective vaccine, we have to consider carefully the following two points: (1) efficient induction of mucosal immunity (2) side effects, such as unwanted inflammation. TLR ligands, such as flagellin for TLR5 ligand and CpG for TLR9 ligand, are widely used as adjuvants for vaccination to enhance the GC reaction[50,56]. However, traditionally, most licensed vaccines administered

parenterally can hardly arouse the mucosal immune response[57]. In our study, oral administration of OVA (antigen) with heat-killed *E. coli* (adjuvant) successfully induced mucosal OVA-specific IgA response (Figure 23). It indicates that heat-killed *E. coli* as an adjuvant may be particularly useful for the development of mucosal vaccines, which are in demand, since most pathogens invade via a mucosal route. Our study showed that non-pathogenic *E. coli* is efficient as mucosal vaccine adjuvant, indicating that our method provides simple and low-cost adjuvant. For the second point, besides the high-cost, another disadvantage of traditional adjuvants is unwanted inflammation. For example, the mRNA vaccine against SARS-COV-2 causes a strong inflammation. To solve this problem, excellent works by modification of CpG have been done to reduce the side effect with intact activity for DC stimulation[58-60]. Since CD11b induction on B cells is independent of DC activation, we expect that heat-killed *E. coli* may be a safe, potent and low-cost adjuvant. Further studies are necessary to answer the questions: how many doses of heat-killed *E. coli* are efficient for enhancing the GC reaction and how is the side effect by comparing with CpG and some other adjuvants. Our results provide new insight into mucosal vaccine development via induction of pre-GC B cells to enhance the appropriate GC reaction.

Chapter 5 Acknowledgement

I really thank Dr. Shinkura for critical comments and technical assistance; Drs. Tomari, Ishii, Ito, and Coban for great comments; Dr. Adachi (Tokyo Medical and Dental University) for great help with in vivo imaging and providing of IgA/Cre-YC3.60 mice; Dr. Kitamura (Tokyo University of Science) for providing 40LB feeder cells; Drs. Morita and Mori and all members in laboratory of immunology and infection control of the University of Tokyo for all their kindness help.

Chapter 6 Reference

1. Frieder D, Larijani M, Tang E, Parsa JY, Basit W, Martin A. Antibody diversification: mutational mechanisms and oncogenesis. Immunol Res. 2006;35(1-2):75-88. doi: 10.1385/IR:35:1:75. PMID: 17003511.
2. Teng, G., & Papavasiliou, F. N. (2007). Immunoglobulin somatic hypermutation. Annu. Rev. Genet., 41, 107-120.
3. Stavnezer, J., Guikema, J. E., & Schrader, C. E. (2008). Mechanism and regulation of class switch recombination. Annu. Rev. Immunol., 26, 261-292.
4. Mesin, Luka, Jonatan Ersching, and Gabriel D. Victora. "Germinal center B cell dynamics." Immunity 45.3 (2016): 471-482.
5. Kurosaki, Tomohiro, Kohei Kometani, and Wataru Ise. "Memory B cells." Nature Reviews Immunology 15.3 (2015): 149-159.
6. Fagarasan, Sidonia, et al. "Adaptive immune regulation in the gut: T cell–dependent and T cell–independent IgA synthesis." Annual review of immunology 28 (2009): 243-273.
7. Chen, Kang, et al. "Rethinking mucosal antibody responses: IgM, IgG and IgD join IgA." Nature Reviews Immunology (2020): 1-15.
8. Ise, W., Fujii, K., Shiroguchi, K., Ito, A., Kometani, K., Takeda, K., ... & Kurosaki, T. (2018). T follicular helper cell-germinal center B cell interaction strength regulates entry into plasma cell or recycling germinal center cell fate. Immunity, 48(4), 702-715.
9. Turner, J.S., Zhou, J.Q., Han, J. et al. Human germinal centres engage memory and naive B cells after influenza vaccination. Nature 586, 127–132 (2020).
10. Andersen, T.K., Huszthy, P.C., Gopalakrishnan, R.P. et al. Enhanced germinal center reaction by targeting vaccine antigen to major histocompatibility complex class II molecules. npj Vaccines 4, 9 (2019).
11. Fagarasan, Sidonia, and Tasuku Honjo. "Intestinal IgA synthesis: regulation of front-line body defences." Nature Reviews Immunology 3.1 (2003): 63-72.
12. Reboldi, Andrea, and Jason G. Cyster. "Peyer's patches: organizing B-cell responses at the intestinal frontier." Immunological reviews 271.1 (2016): 230-245.
13. Wei, Min, et al. "Mice carrying a knock-in mutation of Aicda resulting in a defect in somatic hypermutation have impaired gut homeostasis and compromised mucosal defense." Nature immunology 12.3 (2011): 264-270.
14. Okai, Shinsaku, et al. "High-affinity monoclonal IgA regulates gut microbiota and prevents colitis in

mice." Nature microbiology 1.9 (2016): 1-11.

15. Chen, H., Zhang, Y., Ye, A.Y. et al. BCR selection and affinity maturation in Peyer's patch germinal centres. Nature 582, 421–425 (2020).
16. Ahn, G. O., Tseng, D., Liao, C. H., Dorie, M. J., Czechowicz, A., & Brown, J. M. (2010). Inhibition of Mac-1 (CD11b/CD18) enhances tumor response to radiation by reducing myeloid cell recruitment. Proceedings of the National Academy of Sciences, 107(18), 8363-8368.
17. Ghosn, E. E. B., Yang, Y., Tung, J., Herzenberg, L. A., & Herzenberg, L. A. (2008). CD11b expression distinguishes sequential stages of peritoneal B-1 development. Proceedings of the National Academy of Sciences, 105(13), 5195-5200.
18. Ding, C., Ma, Y., Chen, X., Liu, M., Cai, Y., Hu, X., ... & Yan, J. (2013). Integrin CD11b negatively regulates BCR signalling to maintain autoreactive B cell tolerance. Nature communications, 4(1), 1-13.
19. Zhou, M., Dascani, P., Ding, C., Kos, J. T., Tieri, D., Lin, X., ... & Yan, J. (2021). Integrin CD11b Negatively Regulates B Cell Receptor Signaling to Shape Humoral Response during Immunization and Autoimmunity. The Journal of Immunology, 207(7), 1785-1797.
20. Faridi, M. H., Khan, S. Q., Zhao, W., Lee, H. W., Altintas, M. M., Zhang, K., ... & Gupta, V. (2017). CD11b activation suppresses TLR-dependent inflammation and autoimmunity in systemic lupus erythematosus. The Journal of clinical investigation, 127(4), 1271-1283.
21. Dubois, Bertrand, et al. "Toward a role of dendritic cells in the germinal center reaction: triggering of B cell proliferation and isotype switching." The Journal of Immunology 162.6 (1999): 3428-3436.
22. Lisk, C., Yuen, R., Kuniholm, J., Antos, D., Reiser, M. L., & Wetzler, L. M. (2020). Toll-Like Receptor Ligand Based Adjuvant, PorB, Increases Antigen Deposition on Germinal Center Follicular Dendritic Cells While Enhancing the Follicular Dendritic Cells Network. Frontiers in Immunology, 11, 1254.
23. Komban, R. J., Strömberg, A., Biram, A., Cervin, J., Lebrero-Fernández, C., Mabbott, N., ... & Lycke, N. (2019). Activated Peyer′ s patch B cells sample antigen directly from M cells in the subepithelial dome. Nature communications, 10(1), 1-15.
24. Willis, Simon N., et al. "Transcription Factor IRF4 Regulates Germinal Center Cell Formation through a B Cell–Intrinsic Mechanism." The Journal of Immunology 192.7 (2014): 3200-3206
25. Yang, Z., Sullivan, B. M. & Allen, C. D. C. Fluorescent in vivo detection reveals that IgE+ B cells are restrained by an intrinsic cell fate predisposition. Immunity. 36(5), 857-872 (2012).
26. Nagai, T. et al. Expanded dynamic range of fluorescent indicators for Ca2+ by circularly permuted yellow fluorescent proteins. Proceedings of the National Academy of Sciences. 101(29), 10554-10559, (2004).

27. Yoshikawa, S. et al. Intravital imaging of Ca2+ signals in lymphocytes of Ca2+ biosensor transgenic mice: indication of autoimmune diseases before the pathological onset. Sci Rep. 6, 18738 (2016).
28. Miwa, Y., Tsubota, K. & Kurihara, T. Effect of midazolam, medetomidine, and butorphanol tartrate combination anesthetic on electroretinograms of mice. Molecular vision. 25, 645 (2019).
29. Haniuda, K., Nojima, T., & Kitamura, D. (2017). In Vitro-Induced Germinal Center B Cell Culture System. In Germinal Centers(pp. 125-133). Humana Press, New York, NY.
30. Jolly, C. J., Klix, N. & Neuberger, M. S. Rapid methods for the analysis of immunoglobulin gene hypermutation: application to transgenic and gene targeted mice. Nucleic acids research. **25.10**,1913-1919 (1997).
31. Diamond, M. S., Staunton, D. E., De Fougerolles, A. R., Stacker, S. A., Garcia-Aguilar, J., Hibbs, M. L., & Springer, T. A. (1990). ICAM-1 (CD54): a counter-receptor for Mac-1 (CD11b/CD18). The Journal of cell biology, 111(6), 3129-3139
32. Ager, Ann. "High endothelial venules and other blood vessels: critical regulators of lymphoid organ development and function." Frontiers
33. Kitano, Masahiro, et al. "Bcl6 protein expression shapes pre-germinal center B cell dynamics and follicular helper T cell heterogeneity." Immunity 34.6 (2011): 961-972.
34. Klein, U., Tu, Y., Stolovitzky, G. A., Keller, J. L., Haddad, J., Miljkovic, V., ... & Dalla-Favera, R. (2003). Transcriptional analysis of the B cell germinal center reaction. Proceedings of the National Academy of Sciences, 100(5), 2639-2644.
35. Shinkura, R., Ito, S., Begum, N. A., Nagaoka, H., Muramatsu, M., Kinoshita, K., ... & Honjo, T. (2004). Separate domains of AID are required for somatic hypermutation and class-switch recombination. Nature immunology, 5(7), 707-712.
36. Honjo, T., Nagaoka, H., Shinkura, R., & Muramatsu, M. (2005). AID to overcome the limitations of genomic information. Nature immunology, 6(7), 655-661.
37. Honjo, T., Muramatsu, M., & Fagarasan, S. (2004). AID: how does it aid antibody diversity?. Immunity, 20(6), 659-668.
38. Pasqualucci, L., Bhagat, G., Jankovic, M., Compagno, M., Smith, P., Muramatsu, M., ... & Dalla-Favera, R. (2008). AID is required for germinal center–derived lymphomagenesis. Nature genetics, 40(1), 108.
39. Green, Jesse A., and Jason G. Cyster. "S1PR2 links germinal center confinement and growth regulation." Immunological reviews 247.1 (2012): 36-51.
40. Moriyama, Saya, et al. "Sphingosine-1-phosphate receptor 2 is critical for follicular helper T cell retention in germinal centers." Journal of Experimental Medicine 211.7 (2014): 1297-1305.

41. Gatto, Dominique, Katherine Wood, and Robert Brink. "EBI2 operates independently of but in cooperation with CXCR5 and CCR7 to direct B cell migration and organization in follicles and the germinal center." The Journal of Immunology 187.9 (2011): 4621-4628.
42. Pereira, João P., et al. "EBI2 mediates B cell segregation between the outer and centre follicle." Nature 460.7259 (2009): 1122-1126.
43. Gatto, Dominique, and Robert Brink. "B cell localization: regulation by EBI2 and its oxysterol ligand." Trends in immunology 34.7 (2013): 336-341.
44. Smith, K. G., Light, A., O'Reilly, L. A., Ang, S. M., Strasser, A., & Tarlinton, D. (2000). bcl-2 transgene expression inhibits apoptosis in the germinal center and reveals differences in the selection of memory B cells and bone marrow antibody-forming cells. The Journal of experimental medicine, 191(3), 475-484.
45. Ise, W., & Kurosaki, T. (2019). Plasma cell differentiation during the germinal center reaction. Immunological reviews, 288(1), 64-74.
46. Bąbolewska, Edyta, et al. "Different potency of bacterial antigens TLR2 and TLR4 ligands in stimulating mature mast cells to cysteinyl leukotriene synthesis." Microbiology and immunology 56.3 (2012): 183-190.
47. Borm, M. E. A., et al. "The effect of NOD2 activation on TLR2-mediated cytokine responses is dependent on activation dose and NOD2 genotype." Genes & Immunity 9.3 (2008): 274-278.
48. Watanabe, T., Kitani, A., Murray, P. J. and Strober, W. 2004. NOD2 is a negative regulator of Toll-like receptor 2–mediated T helper type 1 responses. Nat Immunol 5, 800–808.
49. Schwickert, T. A., Victora, G. D., Fooksman, D. R., Kamphorst, A. O., Mugnier, M. R., Gitlin, A. D., ... & Nussenzweig, M. C. (2011). A dynamic T cell–limited checkpoint regulates affinity-dependent B cell entry into the germinal center. Journal of Experimental Medicine, 208(6), 1243-1252.
50. Bode, C., Zhao, G., Steinhagen, F., Kinjo, T., & Klinman, D. M. (2011). CpG DNA as a vaccine adjuvant. Expert review of vaccines, 10(4), 499-511.
51. Chappell, C. P., Draves, K. E., & Clark, E. A. (2017). CD22 is required for formation of memory B cell precursors within germinal centers. *PloS one*, *12*(3), e0174661.
52. Passos, L. S. A., Magalhães, L. M. D., Soares, R. P., Marques, A. F., Alves, M. L. R., Giunchetti, R. C., ... & Dutra, W. O. (2019). Activation of human CD11b+ B1 B-cells by Trypanosoma cruzi-derived proteins is associated with protective immune response in human Chagas disease. Frontiers in immunology, 9, 3015.
53. Caruso, R., Warner, N., Inohara, N., & Núñez, G. (2014). NOD1 and NOD2: signaling, host defense, and inflammatory disease. Immunity, 41(6), 898-908.

54. Medzhitov, R. (2001). Toll-like receptors and innate immunity. Nature Reviews Immunology, 1(2), 135-145.
55. Troy, E. B., & Kasper, D. L. (2010). Beneficial effects of Bacteroides fragilis polysaccharides on the immune system. *Frontiers in bioscience: a journal and virtual library*, *15*, 25.
56. Honko, A. N., Sriranganathan, N., Lees, C. J., & Mizel, S. B. (2006). Flagellin is an effective adjuvant for immunization against lethal respiratory challenge with Yersinia pestis. Infection and immunity, 74(2), 1113-1120.
57. Woodrow, K. A., Bennett, K. M., & Lo, D. D. (2012). Mucosal vaccine design and delivery. Annual review of biomedical engineering, 14, 17-46.
58. Verthelyi, D., Ishii, K. J., Gursel, M., Takeshita, F., & Klinman, D. M. (2001). Human peripheral blood cells differentially recognize and respond to two distinct CPG motifs. The Journal of Immunology, 166(4), 2372-2377.
59. Takeshita, F., Leifer, C. A., Gursel, I., Ishii, K. J., Takeshita, S., Gursel, M., & Klinman, D. M. (2001). Cutting edge: role of Toll-like receptor 9 in CpG DNA-induced activation of human cells. The Journal of Immunology, 167(7), 3555-3558.
60. Ezoe, S., Palacpac, N. M. Q., Tetsutani, K., Yamamoto, K., Okada, K., Taira, M., ... & Horii, T. (2020). First-in-human randomised trial and follow-up study of Plasmodium falciparum blood-stage malaria vaccine BK-SE36 with CpG-ODN (K3). Vaccine, 38(46), 7246-7257.